
Masters Theses

Student Theses and Dissertations

Spring 2016

Silicone hollow fiber membrane bioreactors for mixed aerobic and anaerobic treatment of gas phase toluene and trichloroethylene

Alexander Lee Korff

Follow this and additional works at: https://scholarsmine.mst.edu/masters_theses

 Part of the [Environmental Engineering Commons](#)

Department:

Recommended Citation

Korff, Alexander Lee, "Silicone hollow fiber membrane bioreactors for mixed aerobic and anaerobic treatment of gas phase toluene and trichloroethylene" (2016). *Masters Theses*. 7510.
https://scholarsmine.mst.edu/masters_theses/7510

This thesis is brought to you by Scholars' Mine, a service of the Missouri S&T Library and Learning Resources. This work is protected by U. S. Copyright Law. Unauthorized use including reproduction for redistribution requires the permission of the copyright holder. For more information, please contact scholarsmine@mst.edu.

SILICONE HOLLOW FIBER MEMBRANE BIOREACTORS FOR MIXED AEROBIC
AND ANAEROBIC TREATMENT OF GAS PHASE TOLUENE AND
TRICHLOROETHYLENE

by

ALEXANDER LEE KORFF

A THESIS

Presented to the Faculty of the Graduate School of the
MISSOURI UNIVERSITY OF SCIENCE AND TECHNOLOGY

In Partial Fulfillment of the Requirements for the Degree
MASTER OF SCIENCE IN ENVIRONMENTAL ENGINEERING

2016

Approved by

Mark W. Fitch, Advisor
Joel G. Burken
Glenn C. Morrison

© 2016

Alexander Lee Korff

All Rights Reserved

ABSTRACT

Volatile Organic Compounds (VOCs) are common in effluent waste streams from many sectors of industry and low-cost emission control technologies have the potential to mitigate long-term impacts on the environment. Federal Regulations, such as the Clean Air Act and National Emission Standards for Hazardous Air Pollutants (NESHAPS), as well as state regulations are imposing stricter requirements on point-source emissions, with an emphasis on toxic VOCs. Trichloroethylene (TCE) and tetrachloroethylene (PCE), which are toxic VOCs, have been used since the 1920's for a variety of industrial applications like: degreasing, paint and printing operations, as extraction solvents, and for cleaning and drying cleaning. Microbial degradation of many VOC can be facilitated using hollow fiber membrane bioreactors for a fraction of the cost of traditional control methods. Hollow fiber membrane bioreactors can provide mixed aerobic and anaerobic zones necessary for complete mineralization of alkene chlorinated solvents and allow for greater removal capacity for hydrophobic compounds than typical biological processes. In this work, two silicone hollow fiber membrane bioreactors were operated in parallel to develop loading curves for toluene removal and develop biomass for the subsequent degradation of TCE aerobically and anaerobically. The optimal toluene elimination capacity measured for each reactor varied from 55-60 mg m⁻² hr⁻¹ and no biotic TCE removal was observed.

ACKNOWLEDGMENTS

“A graduate student and their advisor walk into a bar. The advisor orders a rough draft and they sit in awkward silence for eight months.”

I’d like to thank Dr. Fitch for making the last couple years less silent, but a little more awkward. His mentorship and propensity to answer my many questions (sometimes with just a stare) made this project possible and helped me to become the individual I am today. I really do appreciate all his efforts.

Dr. Morrison and especially Dr. Burken were vital for this research project and my academic career as a whole. All the professors’ cooperation in this program makes it feel more like a second family than just an institution.

I would especially like to thank Paul Manley and Melissa Buechlein for helping me overcome my crippling fear of commas and correct spelling. Melissa’s constant support and assistance made this project possible and Paul’s continued editing made this thesis readable.

Lastly, I’d like to thank my family for pretending they understood a single word I have said in the last two years, and always supporting me anyways. For a good night’s sleep please read 1-3 pages of this thesis as needed.

TABLE OF CONTENTS

	Page
ABSTRACT.....	iii
ACKNOWLEDGMENTS	iv
LIST OF ILLUSTRATIONS.....	ix
LIST OF TABLES	xi
 SECTION	
1. INTRODUCTION.....	1
2. LITERATURE REVIEW.....	5
2.1. INTRODUCTION	5
2.2. BIOLOGICAL REACTORS	6
2.2.1. Biofilters.....	6
2.2.2. Biotrickling Filters.	7
2.2.3. Bioscrubbers.....	8
2.2.4. Membrane Bioreactors.	8
2.2.4.1 Mass transfer in membranes.	9
2.2.4.2 Membrane materials.....	10
2.2.4.3 Porous membrane.....	11
2.2.4.4 Dense membranes.....	12
2.2.4.5 Composite membranes.....	12
2.2.4.6 Silicone hollow fiber membrane bioreactor.....	12
2.3. MICROBIAL DEGRADATION OF TOLUENE	13
2.3.1. Aerobic Degradation of Toluene.....	13

2.3.2. Anaerobic Degradation of Toluene.	14
2.4. AEROBIC CO-METABOLISM OF TRICHLOROETHYLENE.....	16
2.4.1. Co-metabolism of TCE in HFMRs with Toluene as a Substrate.	19
2.5. ANAEROBIC REDUCTIVE DEHALOGENATION	21
2.5.1. Evolution of Anaerobic Dehalogenation.....	21
2.5.2. Reductive Dehalogenating Enzymes.....	22
2.5.3. Gibbs Free Energy.....	23
2.5.4. Electron Donors.....	25
2.5.5. Anaerobic Reductive Dehalogenation in HFMRs.....	26
2.6. AEROBIC AND ANAEROBIC ZONES FOR BIOGREDATION	31
3. GOALS AND OBJECTIVES	34
4. METHODOLOGY	37
4.1. OVERVIEW	37
4.2. BIOREACTORS.....	38
4.3. BACTERIAL INOCULUM	41
4.3.1. Aerobic Bacteria.....	41
4.3.2. Anaerobic Bacteria.	42
4.4. ABIOTIC OPERATION	43
4.5. BIOTIC OPERATION	44
4.6. MEASUREMENTS.....	45
4.6.1. Biofilm Thickness.	45
4.6.2. Gaseous Standard Preparation.....	46
4.6.3. Gaseous and Liquid Samples	47
4.6.3.1 Confidence interval.....	48

4.6.3.2 Method detection limit and limit of quantification.	49
4.6.4. Other Analytical Methods.	50
4.6.4.1 pH.....	50
4.6.4.2 Dissolved oxygen.....	51
4.6.4.3 Chemical oxygen demand.....	52
4.6.4.4 Water flowrate.	52
4.6.4.5 Air flowrate.....	53
5. RESULTS AND DISCUSSION	54
5.1. MASS TRANSFER ESTIMATES	54
5.2. PHASE I: TOLUENE DEGRADATION AND LOADING.....	56
5.2.1. Biofilm Growth and Development.	56
5.2.2. Steady-State Toluene Removal.	61
5.2.3. Indigenous Batch Experiments.....	67
5.3. PHASE II: CO-METABOLISM OF TOLUENE AND TCE.....	70
5.4. PHASE III: ADDITION OF REDUCTIVE DEHALOGENATING BACTERIA	74
5.4.1. Subculture Development.	74
5.4.2. Operation.	75
6. CONCLUSION AND RECOMMENDATIONS	80
6.1. OBJECTIVE 1: TOLUENE LOAD AND ELIMINATION CAPACITY	80
6.2. OBJECTIVE 2: AEROBIC TCE CO-METABOLISM.....	81
6.3. OBJECTIVE 3: AERATION.....	81
6.4. OBJECTIVE 4: BATCH TCE AND TOLUENE DEGRADATION.....	82
6.5. OBJECTIVE 5: ANAEROBIC TCE DEGRADATION	83
6.6. OBJECTIVE 6: RDB AND ACETATE ADDITION	83

APPENDIX	85
BIBLIOGRAPHY	95
VITA	103

LIST OF ILLUSTRATIONS

	Page
Figure 2.1 Applicability of various air pollution control technologies.	7
Figure 2.2 Illustration of a cross section of half a hollow fiber membrane bioreactor mass transfer boundary layers shown layers.	10
Figure 2.3 Aerobic Transformation Pathways for Toluene.	15
Figure 2.4 Pathway of anaerobic degradation of toluene	16
Figure 2.5 TCE co-metabolism pathway by toluene degrading bacteria.	18
Figure 2.6 Dehalobacter restrictus specific reductive dehalogenation of PCE cellular interactions.	24
Figure 2.7 Electron Tower adapted from [45].	26
Figure 2.8 Biofilm Substrate and pH gradients from [73].	33
Figure 4.1 Gas phase schematic for bioreactor system.	39
Figure 4.2 Liquid Phase Schematic for Bioreactors.	41
Figure 4.3 Picture of biofilm measurements.	46
Figure 4.4 Toluene Standard Curve.	47
Figure 5.1 Measured biofilm thickness in the growth phase.	58
Figure 5.2 Estimated biofilm volume during growth phase.	59
Figure 5.3 Reactor loading rates and liquid phase toluene concentration during the growth period.	60
Figure 5.4 Dissolved oxygen concentration and pH during growth period.	61
Figure 5.5 Reactor inlet and outlet toluene gas concentrations in the growth period.	62
Figure 5.6 Toluene elimination capacity in reactor 1 and 2.	63
Figure 5.7 Dissolved oxygen concentration and pH during phase I.	65
Figure 5.8 Elimination capacity and pH relationship in phase I.	66

Figure 5.9 Reactor two biofilm thickness and volume.	67
Figure 5.10 Aerobic and anaerobic batch experiments with indigenous bioreactor bacteria.	68
Figure 5.11 Toluene and TCE inlet and outlet concentrations in phase II.	71
Figure 5.12 Toluene elimination capacity in reactors one and two during phase II.....	72
Figure 5.13 Reactor two (aerated) (left) and reactor one (right) (12/6/15).	72
Figure 5.14 Reactor two (left) Reactor one (right) (12/20/15).	73
Figure 5.15 Phase I and II toluene elimination capacities in both reactors.	74
Figure 5.16 Toluene and TCE inlet and outlet concentrations in phase III.	76
Figure 5.17 Toluene elimination capacity in phase I, II, and III.	77
Figure 5.18 Membranes before and after membrane stretching.	78
Figure 5.19 Phase III pH shift over time.	79

LIST OF TABLES

	Page
Table 4.1 Nutrient and trace metal solution.	43
Table 4.2 MDL and LOQ values for GC-FID and GC-MS.....	51
Table 5.1 Mass transfer coefficients adapted from [75].	57

1. INTRODUCTION

Volatile Organic Compounds (VOCs) are common in waste streams in nearly all sectors of industry and long-term use and misuse has resulted in lasting damage to the environment. Common sources of VOCs include dry cleaners, wastewater treatment facilities, petroleum production, landfill or recycling facilities, and painting or coating operations. Stricter regulations are being developed to reduce VOC emissions, with an emphasis on toxic VOCs, like chlorinated solvents and carcinogenic aromatic compounds [1, 2]. Federal Regulations, such as the Clean Air Act and National Emission Standards for Hazardous Air Pollutants (NESHAPS), as well as, state regulations are imposing stricter requirements on point-source emissions. Chlorinated solvents, like trichloroethylene (TCE) and tetrachloroethylene (PCE) have been used since the 1920's for a variety of industrial applications; this has resulted in widespread subsurface plumes which require remediation [3]. Globally, chlorinated solvents are still being used for degreasing, paint and printing operations, as extraction solvents, and for cleaning and drying cleaning. Widespread usage and improper storage and disposal results in thousands of tons of VOC releases into the environment each year.

Most effluent gas or liquid streams contain a mixture of VOCs which can make treatment difficult or expensive. Common methods for controlling VOC emissions can be broken into 3 categories: biochemical, chemical, and physical treatment [2, 4].

Biochemical processes, or biological processes, include biofilters, bioscrubbers, biotrickling filters, and membrane bioreactors. Chemical treatment processes include chemical scrubbers, thermal oxidation, catalytic oxidation, and ozonation. Physical processes are separated into adsorption and absorption treatment options. Biological

process offer many advantages over conventional treatment such as: capital and operational costs, low pressure drop, ability to treat high volumes of air with low concentrations of VOCs, and complete mineralization of pollutants. Biological treatment is often considered more environmentally friendly than other traditional control options [2, 4]. Biological processes use suspended or attached microorganisms to degrade pollutants and the metabolites of degradation. Biofilters, biotrickling filters, and bioscrubbers have been used in industry to treat VOCs and odors emissions for decades and recent research projects have been focused on membrane bioreactors (MBR). Most simple or semi-complex aromatic compounds are readily biodegradable in biological reactors or through *in situ* remediation, but chlorinated solvents are more difficult to biodegrade [3].

TCE and PCE can be degraded by microorganisms both aerobically and anaerobically under certain conditions [3, 5, 6]. Microbial degradation provides a cost effective and an environmentally friendly method for the treatment of chlorinated solvents. TCE and PCE can be degraded by microorganisms through co-metabolism in the presence of a primary substrate [3, 6, 7]. Such aerobic co-metabolism is possible if a substrate is present to provide carbon and energy required for growth of bacteria. Aerobic degradation of PCE or TCE does not provide sufficient energy to support microbial growth and is generally thought to not be a suitable carbon source [5]. Monooxygenase enzymes used during aerobic degradation of a primary substrate also have the potential to metabolize TCE and PCE with no benefit to the microorganism. Many monooxygenases have nonspecific binding sites that allow multiple non-growth substrates to be degraded with no cellular benefit. This differs for anaerobic treatment of halogenated species;

under anaerobic conditions, alkene and some complex and chlorinated hydrocarbons can act as an electron acceptor for microbial metabolism resulting in degradation, this is called reductive dehalogenation or dechlorination [6, 8, 9]. According to estimation of Gibbs free energy, the anaerobic reduction of a chlorinated hydrocarbon will result in 130-180 KJ/mol per chlorine removed, allowing for biomass generation [10]. A mixture of aerobic and anaerobic conditions, and the bacteria able to degrade contaminants, create branched degradation pathways that can result in complete mineralization of TCE [7, 11]. Current research on reductive dehalogenation is focused on *in situ* bioremediation of subsurface chlorinated or brominated hydrocarbon plumes, but this thesis project instead focused on facilitating aerobic co-metabolism and reductive dehalogenation of TCE in two parallel hollow fiber membrane bioreactors (HFMR) [3, 6].

HFMRs consist of a set of fibers or tubular membranes within a liquid filled rigid outside shell, resembling a shell and tube heat exchanger. Gas or liquids with contaminants flow through the inside, or lumen, of the membrane and the contaminants diffuse into a biofilm attached to the outside of the membrane. The outer shell is filled with a liquid mineral salt medium with a variety of nutrients and trace metals that allow for development of a healthy biofilm. The gas and liquid phases in HFMRs are physically separated, which limits mass transfer but allows for high reactor surface area to volume ratios with low pressure drops. The membrane acts as a structure for the biofilm, can allow for compound selectivity, and can limit toxic effects on microorganisms [12, 13]. Membranes are ideal for waste streams containing hydrophobic target compounds due to limitations in cross-phase mass transfer for typical biological reactors [1].

From fall 2015 until spring 2016, two single-tube HFMRs were operated in parallel to investigate the potential for biofilms on silicone membranes to effectively degrade toluene and co-metabolize or reductively dehalogenate TCE over a range of loading rates. The HFMRs were inoculated with an activated sludge-derived culture, and biofilm formed on the membrane under steady operation for about a month. The loading rate and gas residence time (GRT) were varied over a range of low concentrations to develop a loading curve for toluene. The co-metabolic ability of the bioreactors was tested in the winter of 2015, and then the reactors were seeded with two established reductive dehalogenating bacteria (RDB) communities. TCE degradation was tracked for 105 days during co-metabolic and facilitated anaerobic dehalogenation operation. The HFMRs were operated for 215 days to establish long-term operation and to observe shifts in performance or operating parameters.

2. LITERATURE REVIEW

2.1. INTRODUCTION

The Intergovernmental Panel on Climate Change (IPCC) estimates that globally 210 million metric tons of volatile organic compounds (VOCs) are released into the atmosphere each year. Typical VOC pollution control technologies include; air stripping, combustion, sorption, and biological treatment. Biological reactors can effectively remove highly soluble and low molecular weight VOCs such as: methanol, ethanol, aldehydes, acetates, ketones, and many aromatic hydrocarbons [4]. Large volumes of air with low concentrations make conventional treatment uneconomical, but are ideal for biological treatment. Biological reactors rely on the diffusion of contaminants from air to water phase for subsequent microbial degradation. Depending on the system, the rate of diffusion or kinetic degradation rate limits removal. Biological reactors often have lower operating costs but typically have a larger footprint than chemical or physical treatment options. Many chemicals can be biologically degraded through traditional aerobic treatment with common microorganisms, but chlorinated solvents often require a specific microbial culture to facilitate biodegradation. Trichloroethylene (TCE) and tetrachloroethylene (PCE) are chlorinated hydrocarbons that are often used in industry as a degreaser or solvent. For decades chlorinated solvents were used in dry cleaning and industrial processes with little to no restriction or regulation. Global, long-term misuse of TCE and PCE has created many plumes with potential to contaminate ground water and soil for decades. [14-17] Remediation efforts as well as current pollution controls are often focused on chlorinated solvents like TCE.

2.2. BIOLOGICAL REACTORS

Traditional biological reactors for air pollution control (bioscrubbers, biofilters, biotrickling filters) can effectively remove water soluble and low molecular weight VOC's. Large or complex molecules can be difficult to degrade and thus are less suited for biological degradation. Many industrial processes produce high flow waste gas streams that have low gas concentrations that make chemical or physical treatment difficult but are ideal for biological reactors [18]. Conventional biological reactors can have clogging, pH, and nutrient control issues that hollow fiber membrane reactors (HFMRs) can control more readily. HFMRs can provide higher surface area to volume ratios than flat membranes and often have lower pressure drops than other biological systems. Figure 2.1, adapted from Devinny et al. [18], shows the relationship between gas flow and contaminant concentration and which treatment process is best equipped to handle specific waste stream parameters.

2.2.1. Biofilters. Biofilters are bioreactors with a mixed community of fixed-film microorganisms inside a porous-packed bed. The packing media is typically organic material, like wood chips or mulch, which acts as a source of slow-release macro-nutrients, and as a surface for biofilm growth. A gas waste stream is humidified and blown through the packed bed, where the water soluble pollutants partition to the biofilm and are degraded. Biofilms are ideal for treating large volumes of air with low concentrations of VOCs. Biofilters have low operating costs, low capital costs, low pressure drops, and have the capability to treat a wide range and mixture of pollutants.

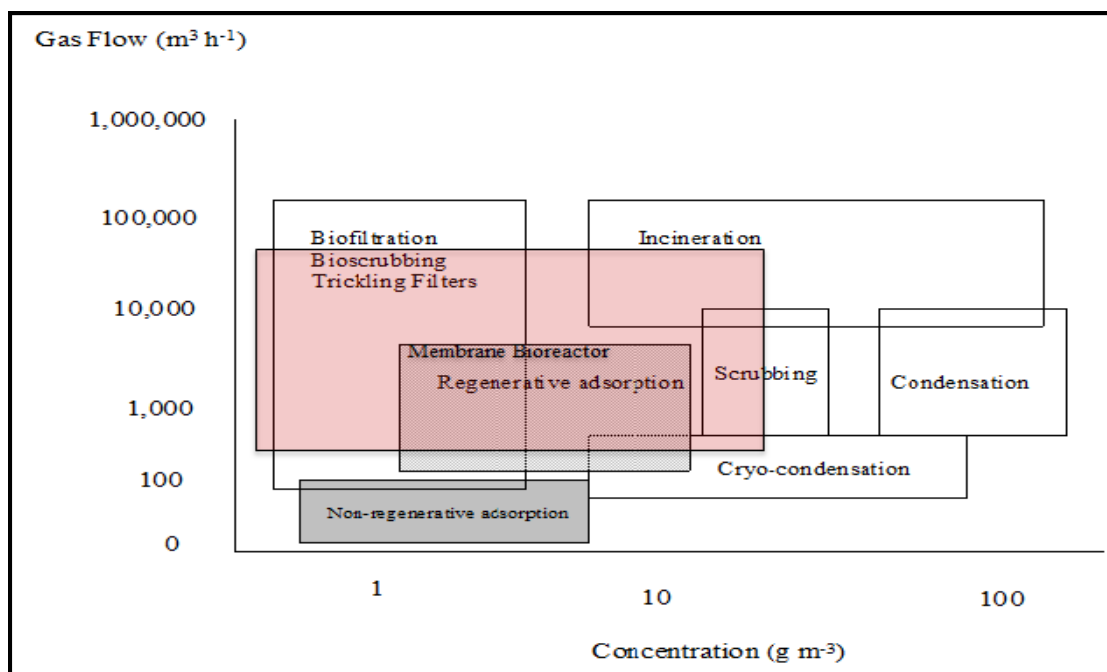


Figure 2.1 Applicability of various air pollution control technologies, adapted from [18].

The main disadvantages of biofilters are clogging due to excessive biomass development, very large footprints, limited degradation of low water soluble compounds, humidity and pH control, and the deterioration of the packing medium.

2.2.2. Biotrickling Filters. Biotrickling filters are similar to biofilters except that instead of humidifying the gas waste stream, a liquid phase is circulated through an inorganic packed bed. The packing media is made of inert substances, like ceramic or plastic, that allow for large surface area to volume ratios with long life spans. The large surface areas allow for larger biofilms to grow, which can lead to higher loading rates than biofilters. Biotrickling filters also have low operating and capital costs, low pressure drops, and the ability to degrade a wide variety of compounds. Biotrickling filters can be

complex to construct and optimal operation can be difficult; excess biomass can form which leads to clogging and increased cost.

2.2.3. Bioscrubbers. Bioscrubbers are typically a two-staged process in which contaminated air is stripped in a wetted packed bed or spray scrubber, and then the liquid is fed into an activated sludge bioreactor. There are many variations on bioscrubbers that try to remove specific pollutants or to increase operating efficiencies. The two-phase system allows the operator better control of functional parameters which often leads to more stable operation. The system has relatively low pressure drop and a smaller footprint than a comparable biofilter or biotrickling filter. The main disadvantages of bioscrubbers are the excess sludge generated and the cost associated with the creation of a secondary liquid waste stream.

2.2.4. Membrane Bioreactors. Over the last 35 years, membrane bioreactors (MBRs) have been used in industry to treat wastewater, and in the last 20 years, research has been focused on using MBRs at the bench scale to treat gas phase VOC emissions [19-22]. Several different configurations of MBRs have been tested including hollow fiber (HFMR), flat sheet, and spiral round reactors. HFMRs are separated into units that use capillary (ID <10mm) fibers and tubular units (ID >10mm) [19]. MBRs create a physical barrier between a contaminated gas phase and a controlled nutrient-rich liquid phase. In the lumen of the bioreactor, gaseous VOCs and oxygen diffuse through the membrane into the liquid phase. Mass transfer in the reactor is driven by concentration gradients and is often the limiting factor in reactor elimination capacity. The membrane acts as a support structure for biofilm growth and suspended microorganisms can grow in

the liquid phase. If complete mineralization occurs, microorganisms degrade the VOCs into CO₂, H₂O, and inert compounds.

2.2.4.1 Mass transfer in membranes. Mass transfer from the gas phase into the liquid phase can be described by Equation 2-1, which can be written over the gas or liquid phase. The overall mass transfer coefficient (K_{ov}) is dependent on the resistance to transfer over each phase in the reactor (Equation 2-2). The regions and boundary layers that limit mass transfer in a MBR are highlighted in . Chemicals in the bulk gas phase must first cross a boundary layer near the surface of the membrane and adsorb to the surface. The diffusion across the membrane is dependent on the membrane material matrix and will be summarized in the next sections. After permeating through the membrane, the chemical has to diffuse through the liquid boundary layer into the bulk liquid phase. Liquid and gas phase mass transfer coefficients can be measured empirically or estimated using correlations.

$$F = K_{ov}A \left(\frac{C_g}{H} - C_l \right) \quad (2-1)$$

$$K_{ov} = \frac{1}{K_{gH}} + \frac{1}{K_{mH}} + \frac{1}{K_b} + \frac{1}{K_l} \quad (2-2)$$

Where:

F is the mass flux through the membrane (g/s)

K_{ov} is the overall mass transfer coefficient (m/s)

A is the membrane area (m²)

C_g is the bulk gas phase concentration (g/m³)

H is the dimensionless gas-liquid partitioning coefficient (g/m³)/(g/m³)

C_l is the bulk liquid phase concentration (g/m³)

K_g is the gas phase mass transfer coefficient (m/s)

K_m is the membrane dependent mass transfer coefficient (m/s)

K_b is the biofilm mass transfer coefficient (m/s)

K_l is the liquid phase mass transfer coefficient (m/s)

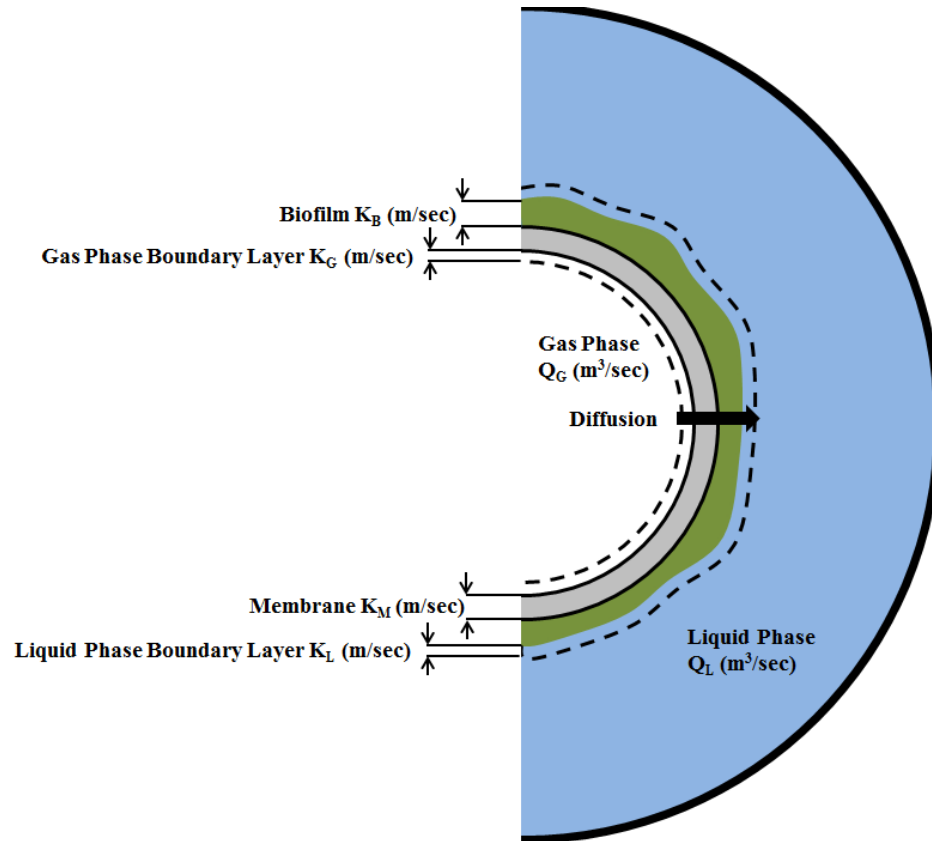


Figure 2.2 Illustration of a cross section of half a hollow fiber membrane bioreactor with mass transfer boundary layers shown layers.

2.2.4.2 Membrane materials. Membrane material and structure determine the biofouling and govern mass transfer in a MBR. Typically, membrane production processes are proprietary and can vary greatly depending on the supplier. Membranes can

be separated into three categories based on the material matrix: dense phase, porous, and composite. Porous membranes have low-permeable, hydrophobic matrix structures with gas filled pores that allow diffusion. Dense phase membranes have a solid material matrix that relies on permeation of a compound into and out of the membrane. Composite membranes have a porous layer for structure with a thin dense phase layer to help reduce biofouling [23].

2.2.4.3 Porous membrane. Porous membranes have a low-permeability matrix structure with pores of diameter between 0.01-1 μm . The small pore size and hydrophobic material prevent water from filling the pores unless critical pressure is reached on the liquid side. Mass transfer in porous membranes is related to the gas diffusivity of a compound in air and can be estimated using equation 2-3. The diffusivity of the chemical in the pores, D (m^2/s), is typically measured, but can be estimated using correlations based on the gas diffusivity. The tortuosity, τ_m , corrects for the pore size and shape. The mass transfer rates in porous membranes are higher than dense membranes but the pores can become clogged by biomass accumulation.

$$K_m = \frac{D\varepsilon}{\tau_m \delta} \quad (2-3)$$

Where:

K_m is the membrane mass transfer coefficient (m/s)

D is the diffusivity of the compound in the pores (m^2/s)

ε is the porosity of the membrane (dimensionless)

τ_m is the tortuosity (dimensionless)

δ is the membrane thickness (m)

2.2.4.4 Dense membranes. Mass transfer in dense phase membranes is dependent on the solubility and diffusivity of chemicals in the membrane matrix. The membrane mass transfer coefficient, K_m , for a dense phase membrane can be estimated using equation 2-4. Fick's first law can be used to estimate mass transfer in a dense membrane. Dense phase membranes have a lower capital cost and lower chance of biofouling than porous membranes, but also have lower mass transfer rates.

$$K_m = \frac{SD_m}{\delta} \quad (2-4)$$

Where:

K_m is the membrane mass transfer coefficient (m/s)

D_m is the diffusivity of the compound in the membrane (m^2/s)

S is the solubility coefficient

δ is the membrane thickness (m)

2.2.4.5 Composite membranes. Composite membranes have both a dense phase and porous phase layer to prevent biofouling and to achieve greater mass transfer rate than a traditional dense phase membrane [19]. A thicker porous layer is used as a support structure for a thin dense phase layer on the liquid side of the reactor. The mass transfer coefficient can be estimated by combining equations 2-3 and 2-4 over the respective phases with a retardation coefficient to account for the interactions where the two layers meet. Composite membranes can have higher surface area to volume ratios than other biological reactors, but the initial construction cost can be as much as 10 times greater [24].

2.2.4.6 Silicone hollow fiber membrane bioreactor. At the bench scale, silicone hollow fiber membrane bioreactors have been used to treat gas phase emissions

of benzene, toluene, ethylbenzene, xylene, 1-butanol, organic sulfur, nitrate, and other VOCs [25-29]. Common VOCs and oxygen have a high permeability in silicone rubber that allows for high mass transfer rates to the biofilm and liquid phase. Work conducted by Attaway et al. [25] on a mixture of BTEX was able to produce elimination capacities similar to porous membrane bioreactors. Low cost silicone tubing can be used to dramatically reduce the cost of HFMR construction and operation.

2.3. MICROBIAL DEGRADATION OF TOLUENE

Toluene pollution is a global issue involving water, land, and air, and microbial degradation is a key factor in the mitigation of emissions. Aerobic degradation of mono-aromatics has been well documented for decades, but anaerobic degradation research is a relatively new field, spanning around 30 years of research. Significant investigation has been conducted to examine the degradation of aromatics, BTEX, and poly-aromatics under low redox conditions. Aerobic degradation of toluene is dependent on a series of oxidase catalyzed reactions for complete degradation and integration into cellular life. Anaerobic degradation of mono-aromatics is often more complex and can be facilitated by multiple metabolic pathways [30].

2.3.1. Aerobic Degradation of Toluene. Aromatic hydrocarbons have a very stable ring structure that require enzyme catalyzed reactions to form more readily degradable central intermediates, like catechol or benzoate, that are more susceptible to ring cleavage. Depending on the location of substituents on the benzene ring, central intermediates are degraded to acetyl CoA, succinyl-CoA, and/or pyruvate.

Under aerobic conditions, toluene is transformed to benzoate by dehydrogenase reactions or to catechol by oxygenase-driven reactions. Figure 2.3, adapted from Fuchs et

al. [30], shows the multiple pathways identified from central intermediates to form useful end products. The direction and rate of degradation is dependent on enzymatic capability of indigenous microorganisms and redox conditions.

2.3.2. Anaerobic Degradation of Toluene. Anaerobic degradation of aromatics is catalyzed by a series of enzymatic reactions to overcome energy barriers [31-35]. The degradation pathways can be separated into four main categories: (1) glycyl radical enzyme catalyzed of fumarate resulting in aromatic-substituted succinates, (2) methylation, (3) dehydrogenase driven hydroxylation of an alkyl species, and (4) direct carboxylation [35]. These reactions can lead to the production of biomass by feeding main metabolic pathways that cause ring saturation, β -oxidation, and/or ring cleavage.

Anaerobic degradation of toluene is the most well studied and understood degradation process of the BTEX compounds [31-33, 35]. Terminal electron acceptors like nitrate, iron (III), manganese, sulfate, and carbon dioxide have all been shown to facilitate degradation of toluene in pure and mixed communities [35]. Anaerobic toluene degradation has been reviewed extensively and all research to date agrees that the first step in degradation is the addition of fumarate on the methyl group of toluene [30-35]. This is a glycyl radical enzyme catalyzed reaction resulting in the formation of benzylsuccinate. The subsequent steps of degradation vary depending on bacterial strain; Figure 2.4 is an example of degradation by denitrifying bacteria [32]. Benzylsuccinate transformation is often completed by the benzoyl-CoA pathway, which leads to ring cleavage and the formation of CO_2 , and has been reviewed by Harwood et al. [34]. Intermediates of toluene metabolism can form through the partial breakdown of the

benzene ring resulting in the formation of acids and alcohols [35]. The anaerobic degradation of toluene leads to the release of hydrogen ions and a shift in pH.

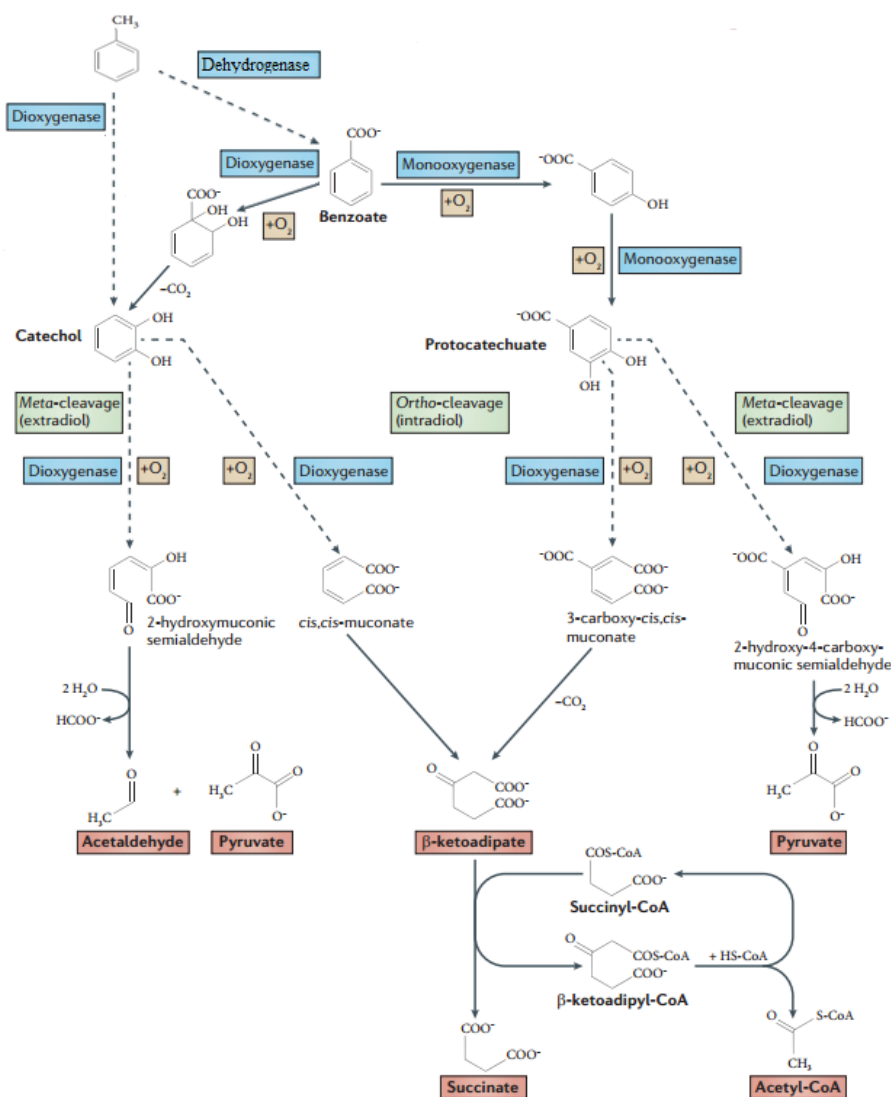


Figure 2.3 Aerobic Transformation Pathways for Toluene. Adapted from [30].

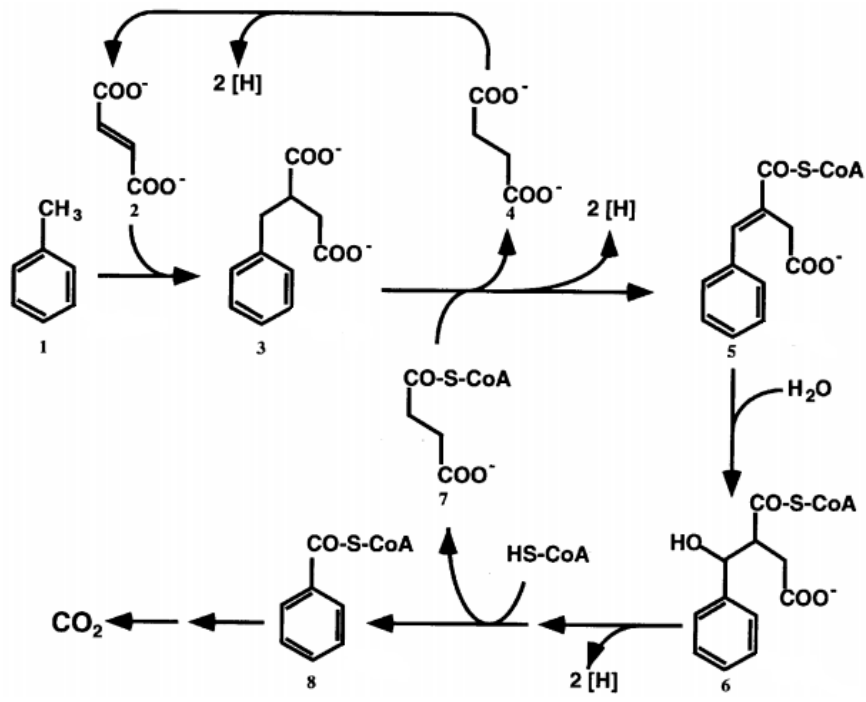


Figure 2.4 Pathway of anaerobic degradation of toluene from [32]) 1) Toluene 2) fumarate 3) benzylsuccinate 4) succinate 5) phenylitaconate 6) 2-carboxymethyl-3-hydroxyphenylpropionyl-CoA 7) succinyl-CoA 8) benzoyl-CoA.

2.4. AEROBIC CO-METABOLISM OF TRICHLOROETHYLENE

TCE can be degraded by microorganisms both aerobically and anaerobically.

Microbial degradation provides a cost effective and an environmentally-friendly method of TCE and other VOC emission reductions. In recent years, focus has been placed on aerobic co-metabolism as a means to initiate *in-situ* and *ex-situ* bioremediation of recalcitrant chlorinated hydrocarbons [3, 36]. It has been theorized that a mixture of aerobic and anaerobic bacteria and conditions create branched degradation pathways that can result in complete mineralization of TCE [7, 11].

Under aerobic conditions, many aliphatic and aromatic hydrocarbon-degrading microorganisms have the capability of degrading select halogenated compounds with non-specific oxygenases. This transformation process is classified as co-metabolism and is dependent on the presence of a primary substrate. Primary substrates are necessary for energy generation and often as a carbon source and include: propane, butane, methane, methanol, nitrate, benzene, phenol, and toluene. The co-metabolized substrate, TCE, does not enter catabolic or anabolic pathways in the cell, but metabolites may. Non-specific mono- or dioxygenases used for primary metabolism attack the TCE carbon double bond forming TCE epoxide. This epoxide is very unstable and can be transformed by abiotic or biotic reactions to dichloroacetate, glyoxylate, formate, and CO₂ [5]. Figure 2.5, from Suttinun et al. [5], highlights the relationship between primary substrate metabolism, toluene, and co-metabolism of TCE by toluene monooxygenase.

Limitations for co-metabolism have been reviewed extensively, but can be summarized by briefly examining inhibition, inactivation, and cytotoxicity [5, 16, 17, 37-39]. Co-metabolism of TCE is dependent on a primary substrate for energy; this can result in competitive inhibition for enzyme activity between the two substrates. Competitive inhibition results in the reduction in substrate utilization rates and can greatly reduce the energy generation in the cells and overall growth. Enzyme inactivation was witnessed in several studies due to damage caused by TCE or metabolites. Varying levels of cytotoxicity were witnessed and seemed to depend on primary substrate and bacterial strain. Toxicity processes like the reduction in cellular respiration, viability, and damage to cellular structure have been related to toxicity induced by TCE degradation [5].

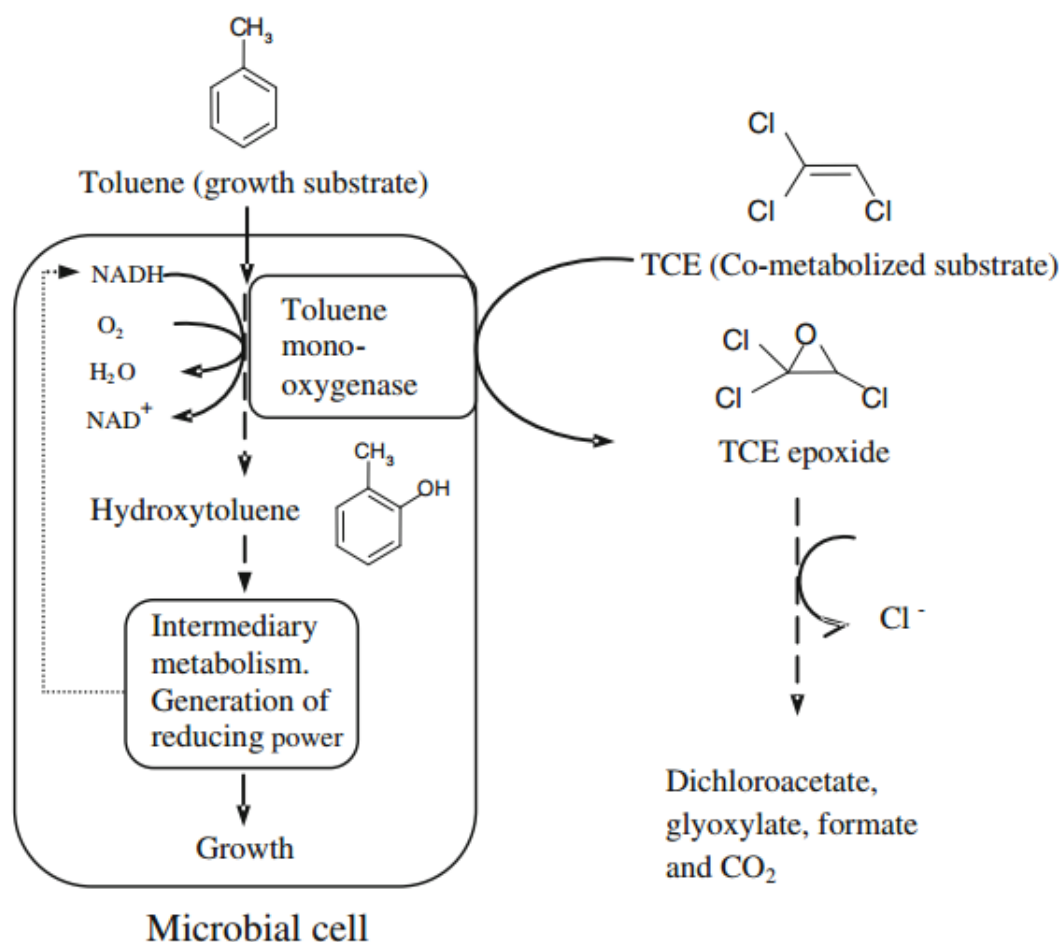


Figure 2.5 TCE co-metabolism pathway by toluene degrading bacteria. Adapted from [5].

Understanding the limiting effects of TCE and other chlorinated hydrocarbons on microbial systems is important for design and implementation of remediation and emission control systems. The capability of substrate specific bacteria to co-metabolize TCE is a relatively new method for treating chlorinated solvents in industry. Modeling specific rates and degradation capacities of microorganisms are integral for selection and design of biological of reactors. In general, TCE had little to no observable acute toxicity

on co-metabolizing microorganisms, but intermediate products can cause structural and enzymatic damage to cells. Chlorinated solvents and intermediate metabolites inhibit and/or inactive enzyme activity for all bacteria communities found in literature. The recovery period varied based upon the strain of bacteria studied and could be mitigated by shifting to steady state operation.

2.4.1. Co-metabolism of TCE in HFMRs with Toluene as a Substrate. There are many reviews on co-metabolism of chlorinated hydrocarbons and this work will summarize the main projects focused on co-metabolism with toluene as a primary substrate in HFMRs [3, 5, 40]. Several different reactor configurations and loading schemes have been tested over the years, all with varying levels of success. HFMRs allow for large surface area-to-volume ratios and membrane selectivity that can optimize co-metabolism [11, 13, 20, 41-43].

In 1995, Parvatiyar et al. [11], operated a HFMR to treat gas phase toluene and TCE. This study was one of the first to investigate the co-metabolism of TCE in a HFMR and the first to explore the potential for mixed aerobic and anaerobic degradation in a single biofilm. The authors grew the biofilm on a gradually increasing toluene load until steady-state was achieved, then added low TCE load to the gas phase. During co-metabolic operations, the HFMR was able to achieve a maximum of 50% removal of TCE relating to an elimination capacity of $0.0092 \text{ g m}^{-2}\text{hr}^{-1}$. The corresponding toluene elimination capacity was $0.032 \text{ g m}^{-2}\text{hr}^{-1}$, which was reduced approximately 10% by the addition of TCE. This project led to additional testing with several different configurations and membrane materials, but was an early attempt at microbial degradation of TCE in a bioreactor.

In 2000, Dolasa and Ergas [41] tested 3 different operating systems for co-metabolism in HFMR to treat gas phase TCE. The authors operated the membrane under mixed TCE and toluene gas phase operation, pulse toluene gas feed, and liquid toluene feed. It was theorized that pulsating toluene load in the gas stream or switching toluene feed to the liquid phase could help to prevent competitive inhibition by separating the substrates and allowing for greater enzyme activity for TCE degradation. The TCE and toluene in gas phase operating system was able to achieve the highest, sustained TCE removal at 36%, a TCE elimination capacity of $0.031 \text{ g m}^{-2}\text{hr}^{-1}$. The related toluene elimination capacity was $0.187 \text{ g m}^{-2}\text{hr}^{-1}$. The HFMR was able to overcome TCE inhibition within 5 days of steady state operation. The alternative loading schemes were unable to achieve higher removal and increased the difficulty in operation.

Zhao et al. [43] investigated the ability of a porous membrane to treat gaseous TCE and toluene emissions over a 9 month study with an anaerobic liquid phase. The reactor was seeded with microorganisms collected from activated sludge that were enriched on toluene. The reactor was operated over a range of loading rates and GRT, but maximum TCE removal was observed with a GRT of 15.7 seconds. The elimination capacity of the reactor for TCE was $0.0016 \text{ g m}^{-2}\text{hr}^{-1}$ relating to a toluene elimination capacity of $0.0116 \text{ g m}^{-2}\text{hr}^{-1}$. The molar toluene to TCE ratio for maximum TCE removal was calculated to be 20:1 under these operating conditions. Co-metabolism could have been limited by the availability of oxygen in this study by decreasing oxygenase activity. The authors reported a continuous increase in pH that seems counter to most other reports in the literature. Competitive inhibition was exhibited by a decrease in toluene

degradation during the initial addition of TCE, but this was overcome within two weeks of operation.

2.5. ANAEROBIC REDUCTIVE DEHALOGENATION

Microorganisms have evolved the capability to dehalogenate aliphatic and aromatic compounds through several different fundamental metabolic pathways [6, 8, 10]. Co-metabolic reactions, catalyzed by either mono- or dioxygenase, can result in the dehalogenation of organohalides in the presence of a primary substrate and oxygen. Under anaerobic conditions, reductive dehalogenase-catalyzed reactions can cause a step cleavage of halogenated species, or the spontaneous cleavage of two halogenated species and the subsequent formation of a double carbon bond. These last two anaerobic processes are classified as substitutive dehalogenation and dehydrohalogenation, respectively. Anaerobic reductive dehalogenation is a dissimulating metabolic process, or energy generating, whereby halogenated species are used as terminal electron acceptors for metabolic electron transfer. The movement of electrons from an electron source, typically hydrogen or acetate, to a halogenated compound results in a net gain in cellular energy through enzymatic metabolism. In works summarized by Fetzner [6], it was found that anaerobic reductive dehalogenation can achieve higher rates of dechlorination than co-metabolic processes.

2.5.1. Evolution of Anaerobic Dehalogenation. Naturally produced and anthropogenic halogenated species present in the environment have caused the evolution of respiratory dehalogenation, as well as oxidative and fermentative mechanisms, to remove organohalides from anoxic areas in the environment [6, 10]. It is known that more than 3500 organohalides are produced naturally, and these natural organohalides

combined with variety of household or industrial products, like solvents and degreasers, have led to a wide spread distribution of persistent halogenated compounds. Complex halogenated compounds like polychlorinated dibenzofurans (PCDF) and polychlorinated dibenzodioxins (PCDD) are formed through natural abiotic events like forest fires and volcanic activity. Many bacteria, fungi, mammals, marine organisms, and higher plants all release a variety of halogenated compounds; chlorinated or brominated alkanes, alkenes, alcohols, ketones, acids, aldehydes, and epoxides have all been found in marine algae. Organisms likely form organohalides to act as chemical defense mechanisms. Biotic halogenated compounds have been shown to act as antibacterial, antifungal, insecticidal, and herbicidal compounds. Even though many halogenated species have an associated toxicity, compounds like chlorinated alkanes, chlorinated alkenes, halogenated benzenes, halogenated phenols, polychlorinated biphenyls, and dioxins have all been degraded by pure or mixed communities of microorganisms. Initially, it was believed that the genes responsible for reductive dehalogenation were a product of modern natural selection due to anthropogenic release of halogenated species, but recent sequencing and the global prevalence of these bacteria has led to a rise in theories regarding ancient evolution related to naturally occurring halogenated species. This shift in thought has occurred mostly within the last two decades [6, 8, 10].

2.5.2. Reductive Dehalogenating Enzymes. Dehydrohalogenase enzymes form double bonds on specific carbon atoms and release HCl through the metabolism of chlorinated alkanes or aromatics [6]. On some polychlorinated aromatics, dehydrohalogenase can catalyze multiple dehalogenating actions, forming multiple carbon double bonds and releasing multiple HCl molecules. Reductive dehalogenases are

enzymes with the capability to facilitate the respiration of halorespiring microorganisms and are associated with substitutive dehalogenation [10]. Multiple studies have found that dehalogenase activity is strongly associated with the cytoplasmic membrane; this can be seen in Figure 2.6 from Hollinger and Schumacher [6, 9]. Figure 2.6 is the proposed dehalogenating respiratory pathway for *Dehalobacter restrictus*. In this pathway, two electrons from hydrogen are transported across the membrane and used by dehalogenase to reduce PCE to cis-DCE.

Chlorine reduction requires one cellular proton which creates a proton motive force that drives ATP synthesis in the cell. The direction of electron flow and location of the dehalogenase varies from strain to strain, but dehalogenation is typically centralized around the cell membrane [6, 10]. Nearly all reductive dehalogenases are monomeric corrinoid-dependent enzymes; cobalt, iron, and B₁₂ are all necessary for the generation of dehalogenase and the anaerobic reductive dehalogenation process [6, 44].

2.5.3. Gibbs Free Energy. Research summarized by Smidt and de Vos [10] shows that Gibbs free energy estimates for the cleavage of halogenated species from aliphatic or aromatic compounds can yield between -130 and -180 kJ/mol of energy per halogenated species removed. This means that halogenated compounds are excellent electron acceptors and dehalogenation can occur in a redox range of 260 – 480 mV, which can be more favorable than sulfate reduction and similar in redox potential to nitrate (NO₃/NO₂) reduction, Figure 2.7 [45]. These estimates also predict that reductive dehalogenation is possible under low aerobic conditions, but rates and prevalence would be low. Modeled growth yields based on these estimates are always well above growth

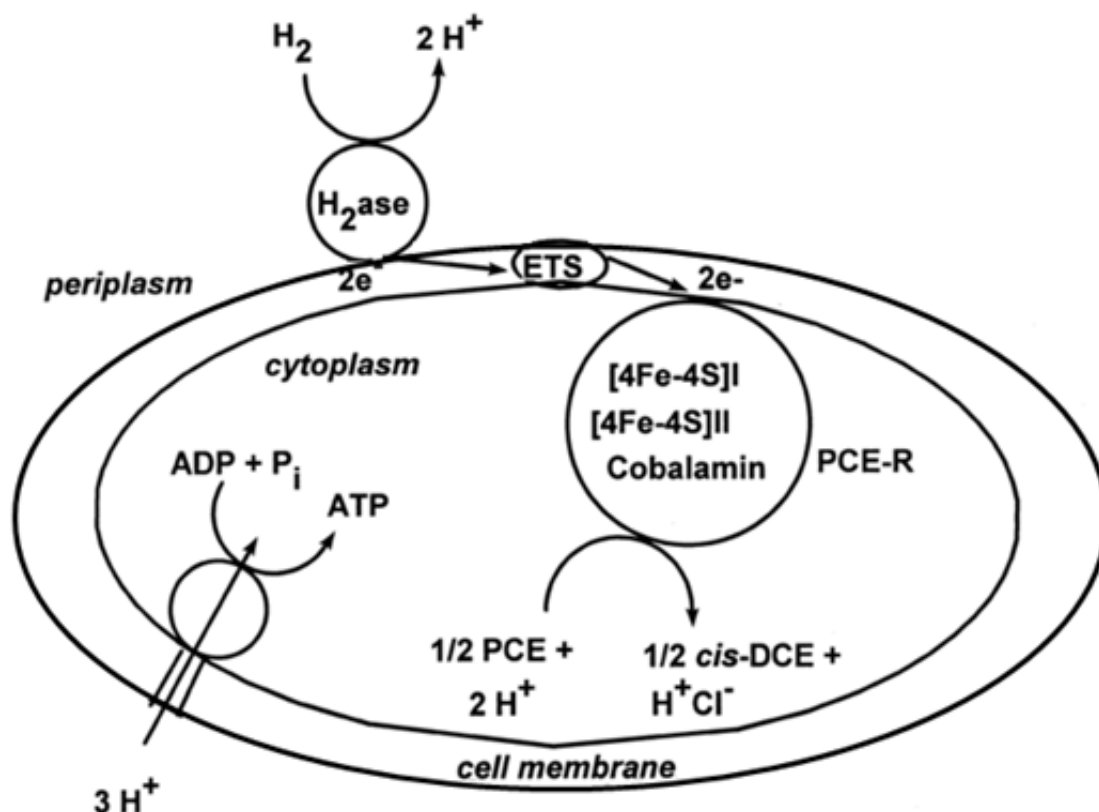


Figure 2.6 *Dehalobacter restrictus* specific reductive dehalogenation of PCE cellular interactions, adapted from [9].

yields observed. This is likely caused by inefficient energy collection due to the slow evolution of existing metabolic pathways involved in dehalogenation.

Gibbs free energy estimates predict that reductive dehalogenating organisms should out-compete other hydrogenotrophic bacteria like sulfate reducers, acetogens, and methanogens when hydrogen is the primary electron source [10, 46, 47]. This means that in mixed communities of hydrogenotrophic microorganisms, reductive dehalogenating organisms should dominate, especially under low hydrogen concentrations [10, 47, 48]. If

excess hydrogenotrophic bacteria are already present in an environment, the growth of dehalogenating bacteria can be severely restricted [48].

2.5.4. Electron Donors. Acetate has also been shown to be a viable source of electrons for some strains of dehalogenating microorganisms [6, 8, 10, 48]. Acetate is formed during the fermentation of organic matter, and this can lead to the net ability of a mixed community to degrade halogenated compounds. Closed electron loops within a microcosm can shift specific microbial populations into syntrophic communities that dehalogenate as an end-product. Work performed by He et al. [48] examined the ability of pure and mixed cultures to use acetate or hydrogen as electron donors for the degradation of PCE, TCE, cis-DCE, and VC[48]. Several strains of dehalogenating bacteria have been isolated that grow on acetate exclusively or as a co-factor in mixed systems [48-50]. All of the acetate-based batch experiments performed by He et al. [48], resulted in the complete mineralization of all chlorinated ethenes in under 14 days. These findings were counterintuitive to previous thoughts on electron donors and helped push further research into the investigation of electron donors on simple and complex halogenated species. He et al. [48] also investigated the mixture of pure strains of acetogenic bacteria and acetate-specific dehalogenating bacteria on the dechlorination of PCE. No acetate accumulation was observed in the system until all electron acceptors were depleted signifying acetogens were directly feeding the dehalogenating bacteria and that acetate-producing bacteria were rate limiting in overall metabolism of chlorinated ethenes. Research has been conducted to investigate the use of mixed, syntrophic organisms and the degradation of chlorinated compounds.

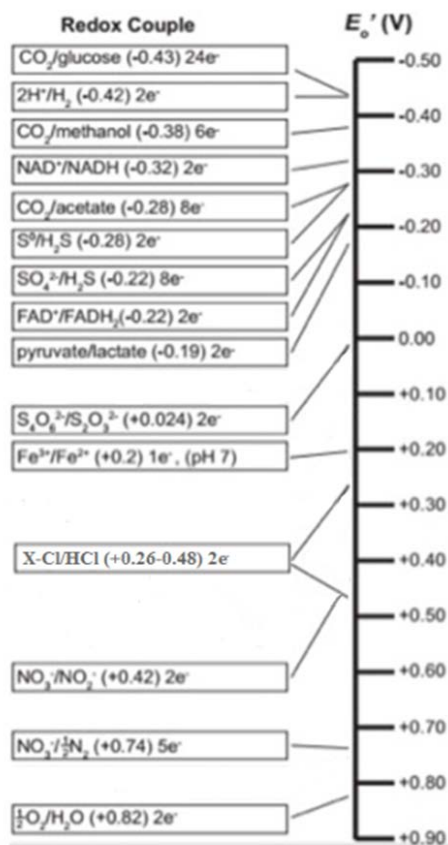


Figure 2.7 Electron Tower adapted from [45].

2.5.5. Anaerobic Reductive Dehalogenation in HFMRs. Typically,

bioremediation of chlorinated solvents is limited to *in-situ* bioaugmentation and biostimulation, however, a variety of bench-scale bioreactors have been tested to allow for *ex-situ* remediation or source control. Bioreactors designed to treat chlorinated solvents can be broken into three categories: aerobic co-metabolic, anaerobic reductive dehalogenating, and mixed or staged bioreactors. Biotrickling filters, up-flow bioreactors, packed bed, batch, and MBRs have all been used to reductively dehalogenate chlorinated solvents with varying success [13, 20, 50-56]. This review will primarily focus on reductive dehalogenation in HFMRs, including configuration and removal capabilities.

Most reported HFMRs designed to facilitate reductive dehalogenation used a similar setup focused on the direct delivery of an electron donor, hydrogen, to a biofilm in the liquid phase of a reactor [46, 49, 57-62]. Typically, HFMRs were designed with non-porous membranes filled with a constant pressure of H_2 ; this configuration was able to overcome the low solubility of H_2 and has been used successfully for denitrification and sulfate reduction [46, 49, 50]. The pressure of H_2 in the membranes was used to control H_2 flux, which could control the formation of hydrotropic bacteria and regulate dehalogenation.

Chung et al. [49] used a premade denitrifying HFMR to dehalogenate TCE to ethene from a continuous liquid stream. The reactor consisted of 32 dense phase membranes with a total surface area of 72.6 cm^2 and volume of 0.52 cm^3 . The HFMR was seeded with biomass from an existing HFMR that had originally been fed PCE and nitrate, but never TCE. During the first 20 days of continuous operation, the biofilm was fed with nitrate as a primary electron acceptor. From day 20 to day 182, the reactor was also fed TCE at a liquid concentration of $7.6\text{ }\mu\text{M}$. By day 150 the reactor was able to convert 93% of the TCE to ethene with no detectable cis-DCE or VC in the effluent. The TCE loading rate was approximately $8.3\text{ mg m}^{-2}\text{ hr}^{-1}$ and the elimination capacity of the reactor was $7.7\text{ mg m}^{-2}\text{ hr}^{-1}$. By analyzing electron fluxes, Chung et al. [49] determined that the conversion of TCE to DCE was rate limiting and most likely caused by the limited bioavailability of H_2 or inhibition from denitrification. These findings were unique due to the fact that most bioreactors were limited by DCE to VC or VC to ethene [50, 51]. DNA and RNA sequencing was used over several intervals in biofilm development to identify the present microorganisms and to quantify gene expression.

DNA sequencing revealed two sets of *Dehalococcoide* bacteria that, when coupled, were able to completely degrade TCE to ethene. DNA and RNA sequencing revealed that these strains were similar to previously identified cultures but not identical. Research suggests that *Dehalococcoide* bacteria strictly use acetate as an electron donor for dehalogenation but not H_2 as a substrate. This means that either *Dehalococcoide* species can use a wider range of electron donors than previously thought, or that the biofilm contained a group of homoacetogens that were capable of producing significant acetate to facilitate dehalogenation. This substrate relationship is a good example of autotrophic and syntrophic communities capable of reductively dehalogenating TCE.

Many bioreactors or bioremediation projects suffered from inhibition when a mixture of chlorinated compounds and daughter products are present. Chung and Rittmann [58] used the same HFMR from the previous experiment to examine the simultaneous reduction of TCE, trichloroethane (TCA), and chloroform (CF). Until a steady state was achieved (~20 days) biomass in the reactors was grown on a mixture of nitrate and sulfate, then the chlorinated species were added to the liquid influent. By day 120 the HFMR was able to degrade all three chlorinated compounds to a fraction of inlet concentrations. The degradation of TCE and TCA greatly increased as effluent CF concentrations decreased. This means that CF or an intermediate metabolite caused some level of inhibition at high concentrations in the reactor. The bioreactor elimination capacity for TCE, TCA, and CF were $7.2 \text{ mg m}^{-2} \text{ hr}^{-1}$, $7.9 \text{ mg m}^{-2} \text{ hr}^{-1}$, and $8.2 \text{ mg m}^{-2} \text{ hr}^{-1}$, respectively. On day 133, the chlorinated solvent load was increased 2.5 times; this resulted in a dramatic increase in intermediate metabolite concentrations from all chlorinated solvents in the effluent.

Karatas et al. [50] studied membrane bioreactors with a similar set-up as Chung et al. [49, 58] with three separate chlorinated solvents as electron acceptors. Each reactor was operated under denitrifying conditions and then fed PCE, TCE, or DCE after biofilm formation. The DCE HFMR was unable to establish any level of dehalogenation and the TCE membrane was limited to TCE to DCE conversion. After 175 days of continuous operation, the PCE HFMR was able to reduce 15% of the PCE to ethene and after 188 days, 95% was reduced to ethene. The effective elimination capacity of the PCE HFMR was $12.8 \text{ mg m}^{-2} \text{ hr}^{-1}$ during optimal operation. During the experiment, the hydraulic retention time (HRT) and H_2 pressure in the reactors were adjusted to reduce intermediate accumulation and to maximize downstream dehalogenation. Karatas et al. [50] found evidence of strictly acetate utilizing bacteria during the molecular investigation of all biofilms. This means that homoacetogenic bacteria were also likely present in their bioreactors. The PCE dehalogenating membrane, from Karatas et al. [50], is another example of a mixed bacterial community facilitating dehalogenation to harmless ethene under anaerobic conditions.

Parvatiyar et al. [11] were the first to attempt to facilitate combined aerobic and anaerobic degradation of TCE in a HFMR. A micro-porous HFMR module was used as the support structure for a heterogeneous biofilm, which allowed for the development of aerobic and anaerobic zones within the reactor. Oxygen was allowed to diffuse through the membrane and oxygenate the biofilm near the surface of the membrane. Acetate, at 7 g/L, was recycled in the liquid phase to stimulate reductive dehalogenation and to create large anaerobic zones in the biofilm and liquid phase. In theory, the anaerobic zone would stimulate the degradation of TCE to cis-DCE and the aerobic zone would allow for

the degradation of DCE to ethene. The reactor was initially run under co-metabolic conditions with toluene as a substrate; this resulted in TCE removal of 50% which equates to a TCE elimination capacity of $9.23 \text{ mg m}^{-2} \text{ hr}^{-1}$. The authors then removed the toluene from the gas phase and reported 35% TCE removal with an elimination capacity of $2.4 \text{ mg m}^{-2} \text{ hr}^{-1}$. These results are interesting because the authors seeded the reactors with activated sludge, which had no reported exposure to chlorinated solvents, and failed to report the addition of the required trace metals or vitamins vital for reductive dehalogenating bacteria (RDB). No batch assays or subsequent biofilm characterization were reported that could prove the presence of RDBs during or following the study. There were also no reports of intermediate metabolite or end product detections during operation, which is unique for the microbial degradation of chlorinated solvents. Complete abiotic mass closure was not established in the bioreactor before operation. The authors assumed less than 1% of the TCE would be lost in the liquid phase due to the low solubility of TCE, but the low liquid-to-gas flowrate ratio in the system would allow for 126% of the gaseous TCE to diffuse into the liquid phase. No liquid TCE concentrations were reported and a net loss of 15% from the liquid recycle, which is within the range reported by other projects, could be used to explain the entirety of the loss from the system.

To date, there have been no complete reports of reductive dehalogenating biofilms in HFMRs to treat aerobic gas streams. Reductive dehalogenating HFMRs have been focused on treating anaerobic liquid waste streams that are contaminated with a variety of chlorinated solvents. This is a useful technology for treating contaminated drinking water or for *ex-situ* remediation of groundwater. Only one previous project has attempted to

facilitate complete mineralization of chlorinated solvents from an aerobic gas stream, and that work failed to fully establish mass closure or show the presence RDBs. This thesis project is an attempt to facilitate reductive dehalogenation in a mixed biofilm in a HFMR designed to treat a mixture of VOCs from an aerobic gas stream.

2.6. AEROBIC AND ANAEROBIC ZONES FOR BIOGREDATION

Anaerobic reductive dehalogenation of PCE and TCE is more energetically favorable than DCE or VC and some organisms lack the ability to degrade DCE or VC. These issues often lead to a bottle-neck, or limiting, effect for the complete mineralization of highly chlorinated solvents in biological reactors or during *in-situ* bioremediation [6, 48, 49, 58]. To combat this issue, stage reactors have been tested and used in the field to completely degrade PCE and TCE to ethene by separating anaerobic and aerobic bacteria [6, 55, 63-67]. In anaerobic reactors, accumulation of VC results in toxic inhibition on microorganisms and even results in complete reactor failure, but coupled aerobic reactors allow for complete conversion of TCE, DCE, and VC. Many authors found that the transformation of DCE and VC were still rate limiting within the reactors due to slow conversion rates by aerobic bacteria [6, 63, 64, 66]. Staged bioreactors have higher initial capital cost than a single reactor and added a complexity to design, so coupled aerobic and anaerobic degradation in a single reactor or biofilm would be the ideal treatment option for chlorinated solvents [7, 11].

The limited diffusive transport and complex heterogeneity in biofilms can lead to steep substrate and nutrient gradients that allow for mixed transformation of compounds by different, but often syntrophic pathways [68-70]. Heterogeneous biofilms are often filled with channels or voids that can create microcosms of chemical/nutrient pockets due

to increased or decreased mass transfer [71]. The general heterogeneity of biofilms makes modeling difficult and often leads to the assumption of homogeneity in stratified layers within the biofilm, perpendicular to the surface. Chemical gradients in biofilms are formed by limited mass transfer rates coupled with high substrate utilization rates and have been well documented in many nitrifying and denitrifying biofilm studies [72-74]. Schramm et al. [73] used microsensors and fluorescence *in situ* hybridization (FISH) to track substrate gradients and identify microorganisms in a coupled nitrifying-denitrifying membrane bioreactor. The microsensors allowed the authors to track O_2 , NO_3 , NO_2 , and NH_4 in the biofilm and bulk liquid phase over several weeks of operation. High rates of ammonia conversion in the biofilm near the membrane led to a steep oxygen gradient resulting in the formation of an anoxic zone within the biofilm, ranging from 200-600 μm from the membrane surface, Figure 2.8. The anoxic zone near the bulk liquid allowed for conversion of nitrate and nitrite and the aerobic zone allowed for the transformation of NH_4 and NH_3 . Stratified layers of microorganism were identified within the biofilm using FISH that further illustrate the competitive advantage of some organisms. Mass transfer models coupled with substrate and co-substrate models can be used to estimate aerobic and anaerobic zones, as well as, reactor elimination capacity.

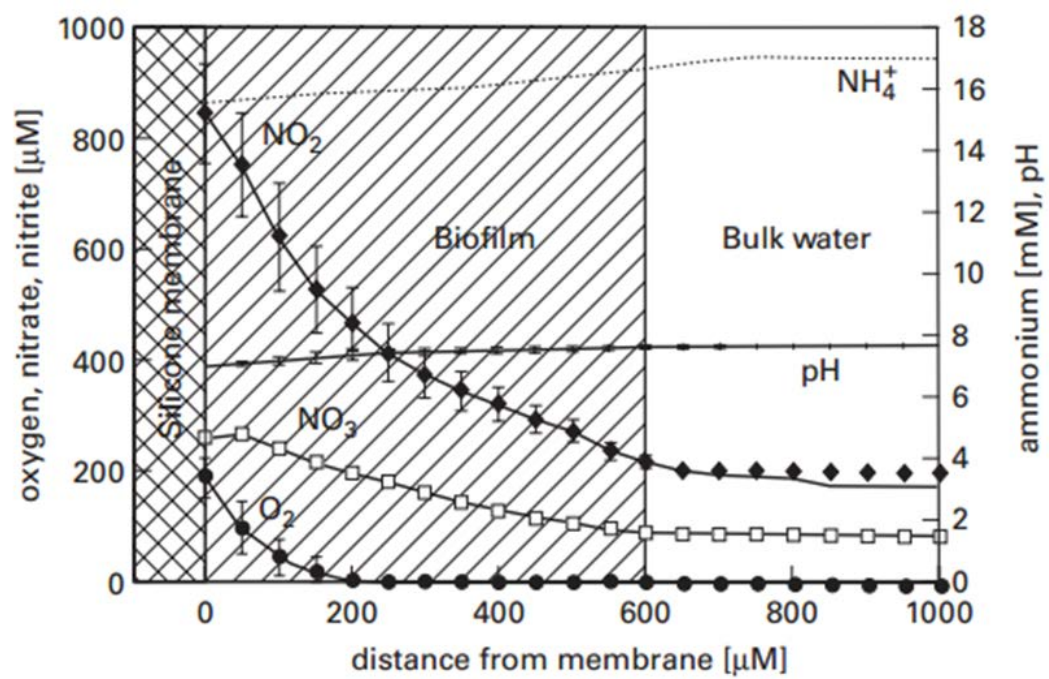


Figure 2.8 Biofilm Substrate and pH gradients from [73].

3. GOALS AND OBJECTIVES

The goal of this research project was to investigate the potential for VOC control using silicone hollow fiber membrane bioreactors. This project also tried to investigate the ability of a single biofilm to facilitate mixed aerobic and anaerobic zones for the complete biodegradation of chlorinated solvents from aerobic gas streams. To achieve these goals, the following objectives were formulated:

- Objective: Operate two single tube hollow fiber membrane bioreactors over a range of loading rates and gas residence times (GRTs) to develop loading-elimination capacity (EC) curves for the biodegradation of a single stream of toluene.
 - Hypothesis tested: The HFMRs will be able to treat toluene over a range of loading rates. Adjusting the GRT will affect the driving force into the membranes, which will affect the EC.
- Objective: Quantify TCE co-metabolism in the HFMR over a range of loading rates and primary and secondary substrate molar ratios. Track shifts in toluene degradation during this phase and compare to single substrate operation.
 - Hypothesis tested: The toluene-degrading biofilm will be able to co-metabolize TCE at a low rate. Increasing the molar ratio of toluene to TCE will increase TCE removal in the reactors. The addition of TCE to the system will decrease the toluene EC in the reactors.
- Objective: Measure TCE and toluene removal with the addition of aeration to the liquid phase of a reactor.

- Hypothesis tested: Oxygen-limiting conditions exist in the liquid phase and outer biofilm so that the addition of aeration in the liquid phase will increase toluene and co-metabolic TCE removal.
- Objective: Use batch experiments with indigenous biofilm bacteria to confirm aerobic toluene and TCE degradation. Deoxygenate a portion of the indigenous bacteria and test the anaerobic degradation of TCE with the addition of acetate as an electron donor.
 - Hypothesis tested: The biofilm bacteria are able to degrade toluene and co-metabolize TCE under aerobic conditions. It was theorized that no dehalogenating bacteria (RDB) would be present in the biofilm and therefore no anaerobic TCE degradation will occur.
- Objective: Investigate the possibility of reductive dehalogenation in a heterogeneous biofilm used to treat an aerobic gas stream.
 - Hypothesis tested: The high oxygen mass transfer into the biofilm will prevent anaerobic conditions in the biofilm or liquid phase. Because RDBs require anaerobic or microaerophilic conditions to survive, RDB activity will not be present. The buffering capacity of the liquid media will be sufficient to maintain the proper pH range for RDBs.
- Objective: Investigate the addition of acetate as an electron donor to increase the anaerobic regions in the biofilms and as a source of electrons for reductive dehalogenation. Add established RDB to the liquid phase of the reactor and measure TCE removal.

- Hypothesis tested: Increased BOD has the potential to increase overall anaerobic zones in the biofilm and decrease the ambient dissolved oxygen concentration in the liquid phase, thus promoting the activity of RDB. The addition of a secondary primary substrate (acetate) will reduce the toluene degradation in the reactors. The addition of a secondary primary substrate (acetate) will reduce the toluene degradation in the reactors but enhance TCE reductive dehalogenation by RDB added to the system.

4. METHODOLOGY

4.1. OVERVIEW

Two single tube hollow fiber membrane bioreactors (HFMRs) were operated in parallel to develop loading curves for toluene degradation and to investigate trichloroethylene (TCE) degradation. The reactors were operated to test co-metabolism of TCE in the presence of toluene and to test the ability of reductive dehalogenating bacteria (RDB) to function in a partially aerobic biofilm. The project was also designed to test the ability of mixed biofilms to facilitate simultaneous aerobic/anaerobic degradation of TCE and the by-products of degradation (DCE and VC), which are often rate limiting. Furthermore, the addition of acetate as an electron donor and source of biochemical oxygen demand (BOD) was studied in an attempt to increase anaerobic zones in the biofilm and increase reductive dehalogenation potential. The bench-scale bioreactors each consisted of one silicone tube submerged in a nutrient rich liquid phase under low flow recirculating conditions. Inlet and outlet gas and liquid samples were measured using gas chromatography during biotic operation and to determine abiotic mass closure. During the enhanced anaerobic operation (phase III), chemical oxygen demand (COD) was measured to estimate the degradation rate of the aqueous acetate. Throughout the growth and initial operating phases the tubular membranes were projected onto a nearby white screen to estimate *in situ* biofilm thickness. Temperature, dissolved oxygen, pH, and gas and liquid flowrates were all monitored during operation.

4.2. BIOREACTORS

Each HFMR, illustrated in Figure 4.1 and Figure 4.2, consisted of a Pyrex glass cylinder with twist-off rubber stoppers, from Plasticoid Company (part # L9M669), capping each end. Steel tubing with outer diameter of $\frac{1}{4}$ inch was inserted through the rubber stoppers and used to secure the membrane and to provide inlet and outlet liquid sampling ports for the reactors. Peroxide-cured silicone, $\frac{1}{4}$ inch ID x $\frac{3}{8}$ inch OD, from Cole-Parmer (item# WU-06411-71) was used as the tubular membrane in each reactor. The membrane was secured by Swagelok[®] ferrules that were press fit onto the steel tubing pieces which had been inserted into the rubber stoppers. The ferrules acted as a hose barb for the membranes that allowed easy assembly and kept the membranes taut during installation and operation. Teflon[®]-lined silicone rubber septa were placed inside $\frac{1}{4}$ inch Swagelok[®] caps and used to seal the liquid sample ports on the top and bottom of the reactors.

Figure 4.1 is a schematic of the gas phase for the bioreactor system. Compressed air was supplied from the university's gas system, a Bellofram Corporation regulator (part# 241-980-066) maintained the pressure at a constant 16 psi, and the total flow was controlled by a Cole-Parmer Valved Acrylic Rotameter (Item# EW-32461-50). The flow then split into 3 parallel lines, each controlled by a 316 Stainless steel needle-valve with Yor-Lok tube fittings from McMaster-Carr (part # 45585K85). Two of the three lines, were forced through separate flasks, sealed with rubber stoppers, each containing a 40 mL vials of the pure, liquid VOC, TCE or toluene. Once steady state was achieved in the flask, the VOC vials had a constant emission rate that allowed for very controlled loading over an extended period of time. Aluminum foil, with a set number of tiny holes, was

secured to the vials containing the VOCs and used to control the emission rate. After each flask, a 316 stainless steel ball-valve from Swagelok® (part # 463836001) was placed inline; this gave the operator the ability to completely remove a VOC with very little effort. Following the ball-valve, each contaminated line had a low flow Cole-Parmer Valved Acrylic Rotameter (Item# EW-32461-40), which allowed for rough control of the loading during operation.

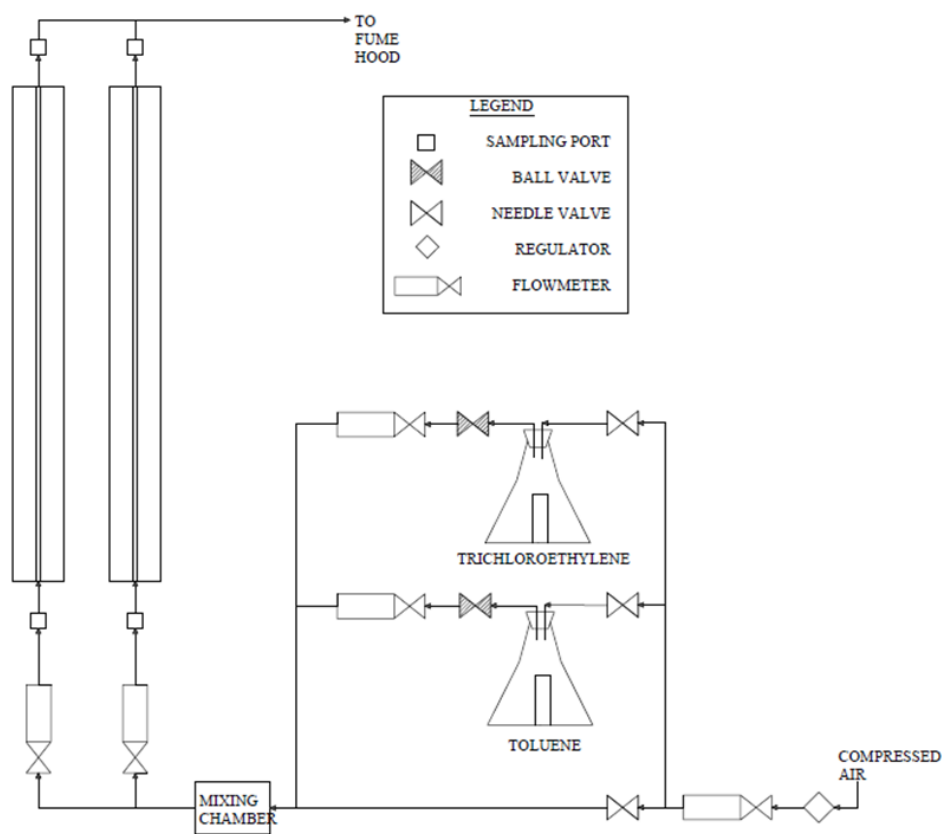


Figure 4.1 Gas phase schematic for bioreactor system.

All three lines were then rejoined and sent to a Bimba stainless steel (mixing) chamber to improve mixing by increasing the volume and dramatically reducing gas phase velocity. After the mixing chamber, the flow was split and piped to the top of each bioreactor and controlled by two Cole-Parmer Valved Acrylic Rotameters (Item # WU-32460-42). Teflon[®]-lined silicone rubber septa were placed inside 1/4-inch Swagelok[®] caps and placed inline before and after the bioreactors as gas phase sampling ports.

Figure 4.2 is the liquid phase schematic for the two membrane bioreactors. Liquid flow was a constant 10 mL/min entering from the bottom and exiting the top of each reactor. The liquid was pumped through the bottom and exited the top of the reactors to allow for removal of all air bubbles from the system, to allow for easier draining of the reactors, and to limit the potential for clogging in the recycle lines. Having the liquid phase enter through the bottom instead of top prevented setting suspended solids from clogging the exit, and allowed gravity to help filter the recirculating liquid. The recycle lines were flexible, clear, Tygon[®] tubing, and Cole-Parmer MasterFlex[®] tubing was used inside of the pump. That pump was a multi-head peristaltic pump (Cole Parmer Instrument Company, Model 7553-85) with Masterflex speed controller (Cole Parmer Instrument Company, Model 7553-71, 50/60 Hz, 115 V, and 3 Amp), which was used to circulate the liquid phase in both reactors. The reservoir, tubing, and reactor combined to a liquid phase volume of 750 mL.

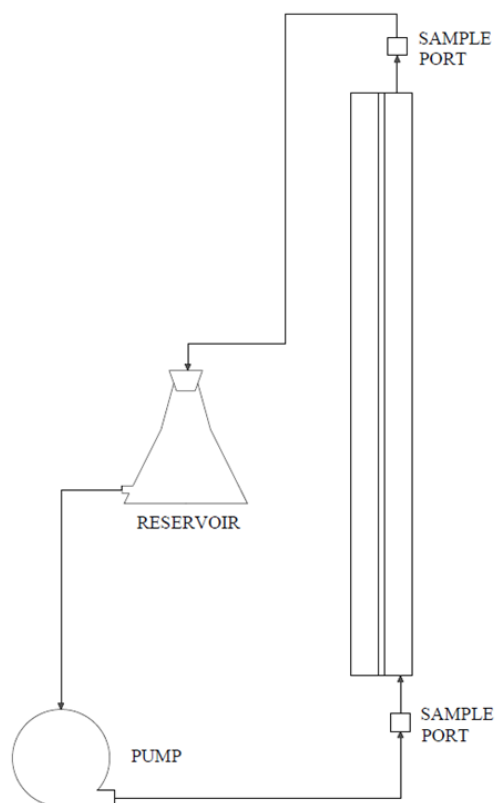


Figure 4.2 Liquid Phase Schematic for Bioreactors.

4.3. BACTERIAL INOCULUM

4.3.1. Aerobic Bacteria. During the spring of 2015, an Erlenmeyer flask was seeded with return activated sludge from the Rolla, MO southeast wastewater treatment plant and placed on an orbital shaker. The flask was fed a mixture of glucose and toluene to a concentration of 15 mg/L each. This was done to provide a ready carbon sources and promote growth of toluene-oxidizing bacteria. Aluminum foil was used to cover each flask and the headspace was routinely analyzed for toluene to determine the dosing

schedule. After initial biomass accumulation, a subculture was seeded with 1% by volume of the culture and supplied with nutrients adapted from England et al. [75]. The subcultures were then placed on the same orbital shaker with only toluene as a carbon source. The nutrient solution, shown in Table 4.1, was adjusted using ratios found in Kim et al. [76] and Sui et al. [15] to allow for greater buffering capacity and to supply a wider range of trace nutrients. The trace-elements were stored in a separate solution at a concentration requiring 1 mL/ L of primary solution and mixed following method 7.5.9 from Methods for General and Molecular Microbiology 2nd edition [77].

4.3.2. Anaerobic Bacteria. Several attempts to culture new or subculture existing dehalogenating bacteria failed in the spring and summer 2015. In fall 2015, two different dehalogenating samples were obtained and subcultured and shown to degrade PCE in batch cultures before inoculation into the HFMRs. A sample of *Dehalococcoides mccartyi* from Terra systems and a mixed dehalogenating consortium from TSI were subcultured using methods from Löffler et al [78]. A 100-fold salt solution was prepared with 100 g/L NaCl, 50 g/L MgCl₂ X 6H₂O, 20 g/L NH₄Cl, 30 g/L KCl, and 1.5 g/L CaCl₂ X 2 H₂O. A vitamin solution was substituted with a concentrated yeast extract solution of 1 g/L. A 2-L Erlenmeyer flask with 900 mL of distilled water was placed on a stir/heating plate and 10 mL of the 100-fold solution was added. One mL of the trace metal and vitamin solutions were added followed by a resazurin solution. Acetate was added as the electron donor to a concentration of 30 mM. The solution was filled to 1 L with more distilled water and brought to a boil for 10 minutes. The solution was then cooled in an ice bath and placed inside an anaerobic glovebag. All remaining dissolved oxygen was eliminated by bubbling pure N₂ through the media for approximately an hour, and then

Table 4.1 Nutrient and trace metal solution.

Aerobic Media		Trace Metals	1:100
Chemical	mg/L	Chemical	mg/L
(NH ₄) ₂ SO ₄	2000	ZnSO ₄	100
K ₂ HPO ₄	750	H ₃ BO ₃	50
KH ₂ PO ₄	750	CuSO ₄ *6H ₂ O	40
		CoCl ₂ *6H ₂ O	50
		MnCl ₂ *4H ₂ O	500
		NiCl ₂ *6H ₂ O	45
		Na ₂ MoO ₄ *2H ₂ O	1000
		MgSO ₄	1500
		FeSO ₄ *7H ₂ O	500
		CaCl ₂ *2H ₂ O	1500

Na₂S to a concentration of 0.2 mM was added as a free-oxygen scavenger. The pH was adjusted using 1 M NaOH to 7.25. While in the glovebag, 100mL of media was placed in two 260 mL amber glass bottles with Mininert[®] caps. A 1% by volume solution of each of the dehalogenating communities was used to start two subcultures. A 90% N₂ and 10% H₂ gas stream was used to bring the bottle headspace to approximately 5% H₂. The bottles were placed on an orbital shaker and PCE degradation was measured over two weeks. Once significant biomass had accumulated, the HFMRs were seeded with both subcultures with a 1% by volume inoculant.

4.4. ABIOTIC OPERATION

Abiotic mass closure and the steady state equilibrium time were measured for TCE, toluene, and the mixture of TCE and toluene during stagnant and recirculating

conditions for both bioreactors. Inlet gas, outlet gas, and liquid sample concentrations were checked periodically and mass closure was estimated for each system using equation 4-1. Under stagnant conditions mass closure was approximately 97% for TCE, toluene and a mixture of the two and occurred after approximately 11 hours. Under recirculating conditions, mass closure was estimated at $94-95 \pm 7\%$ with some increased loss in the liquid phase most likely through the permeable liquid recirculation lines. The time to apparent steady state under recirculating conditions, 2-3 days, was significantly longer than under stagnant conditions. During abiotic operation, flow through the VOC flasks was shut off and the outlet concentration was measured while pure air passed through the membranes. After approximately 11 hours the concentration in both reactors dropped below the quantifiable level but was above detection level, and after 18 hours the air was considered free of VOCs.

$$\text{Mass Closure (\%)} = \frac{Q_{\text{Air}}C_{\text{AirOut}} + Q_{\text{Liquid}}C_{\text{LiquidOut}}}{Q_{\text{Air}}C_{\text{AirIn}} + Q_{\text{Liquid}}C_{\text{LiquidIn}}} \times 100$$

4.5. BIOTIC OPERATION

After abiotic experimentation was completed, the bioreactors and reservoirs were filled with the nutrient media used during initial enrichment of the aerobic bacteria and recirculation was started. A low toluene load was introduced to each bioreactor and the system was allowed to reach quasi-steady. This allowed for the accumulation of toluene in the liquid phase, which agreed with Henry's law estimates. The reactors were then each seeded with a 1:100 mL ratio of aerobic biomass subculture, through the liquid sample port directly into the shell side of the reactors.

The bioreactors were operated through three phases: Phase I-toluene degradation, Phase II-aerobic co-metabolism of TCE, and phase III enhanced anaerobic degradation with acetate addition in the liquid phase. The toluene phase started with a growth phase to create the initial biomass on the membranes and then to establish loading curves for the bioreactors under very low loading conditions. After an initial quasi-steady state was reached (30 days); the loading rate and gas resident time (GRT) were varied and elimination capacities were determined. During the second phase, TCE was added to the air phase and co-metabolic removal was measured for a variety of loading rates. During phase II the liquid phase in reactor two was aerated using an aeration stone to saturation (~8.4 mg/L) in the reservoir to correct for the limited oxygen availability. During the final phase of operation, acetate and dehalogenating bacteria were added to the reactors in an attempt to improve anaerobic degradation of TCE.

4.6. MEASUREMENTS

4.6.1. Biofilm Thickness. The biofilm thickness was measured using a BESELER™ PS 360 projector and gridded screen located one meter away, Figure 4.3. A piece of membrane was submerged in water for an extended period of time to mimic the swelling of the membrane in the bioreactor during operation. The swelled membrane piece was measured and used to scale the measurements of the biofilm on the screen with the measured projected biofilm. Measurements for the biofilm were taken at twelve equidistant heights along on the membranes. During the initial growth phase, biofilm measurements were taken routinely for both bioreactors. After significant biomass was established, biofilm thickness was measured for reactor two to quantify biomass with different load rates and GRTs and during the last two phases of operation.



Figure 4.3 Picture of biofilm measurements.

4.6.2. Gaseous Standard Preparation. Toluene and TCE standards for use with the gas chromatograph (GC) were prepared with distilled water and certified HPLC grade chemicals. Saturated water stock solutions of TCE and toluene were used to make all standards. Measured amounts of TCE- and toluene-saturated water solution were added to 100 mL of distilled water in 260-mL bottles with Mininert[®] caps to create a range of standards with the desired headspace and liquid phase concentrations. Standards were shaken vigorously and then placed on an orbital shaker for a minimum of an hour to allow for equilibrium. Solubility constants, from Amoore and Hautala [79], were used for all calculations and reported for TCE and toluene as 1.1 g/L and 0.54 g/L, respectively. Headspace concentrations were calculated for standards using temperature corrected Henry's law constants from Staudinger and Roberts [80] and equation 4-2 and 4-3. The dimensionless Henry's law constant, at a temperature of 21°C, for TCE and toluene were found to be 0.347 and 0.229, respectively. Standards were analyzed, plotted, and fitted

with a liner curve. Figure 4.4 is an example of a standard curve used to estimate inlet and outlet gas and liquid concentrations.

$$M_{Total} = C_{Air}V_{Air} + C_{Liquid}CV_{Liquid} \quad (4-2)$$

$$K_H = \frac{C_{Air}}{C_{Liquid}} \quad (4-3)$$

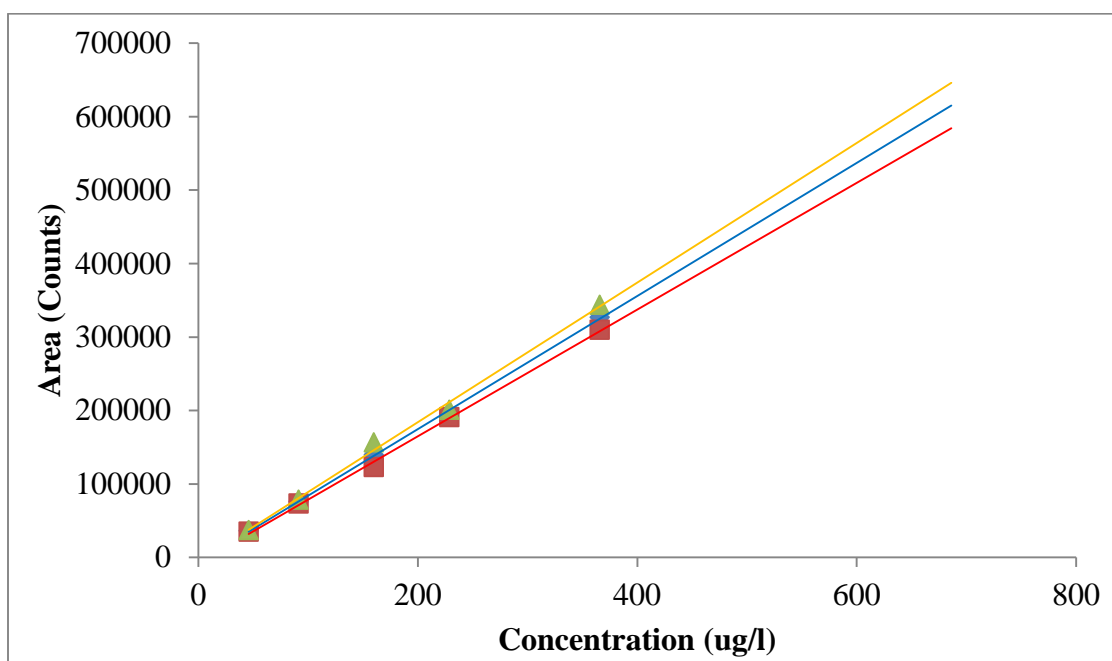


Figure 4.4 Toluene Standard Curve.

4.6.3. Gaseous and Liquid Samples. Gas samples were collected using a 250- μ L Hamilton™ 1700 series GasTight™ SampleLock™ syringe (part# 14-815-564.) Liquid samples were collected using a 10-mL Hamilton™ model 1010 GasTight™ syringe with Luer Lock (part# 81601.) The 10-mL liquid samples were placed in a 40-mL glass vial,

capped with Mininert[®] caps, and biological activity was neutralized with 20 μL of 5N H_2SO_4 , then samples were placed on an orbital shaker and allowed to equilibrate. After equilibration, headspace over the liquid samples was analyzed and the liquid phase concentration was calculated using the appropriate Henry's law constant.

During most of phase I and III, a Hewlett Packard 5890 Series II Gas Chromatograph with Flame Ionization Detector and a J&W Scientific HP-5 (30 m, 0.32 mm ID, and a 0.25 μm film thickness) was used to analyze headspace and gas samples. The GC-FID was operated under a split-less mode with a nitrogen flow of 18 mL/min and isothermally at a temperature of 50 $^{\circ}\text{C}$. Toluene and TCE eluted at 2.2 and 1.7 minutes, respectively. The inlet and detector were held at 250 $^{\circ}\text{C}$ during all runs.

During parts of phases I, II, and III, an Agilent 5793 Network Mass Selective Detector (GC-MS) was used to analyze gaseous samples. The GC-MS was operated with direct headspace injections and a gas 1:40 split. The column flow rate was 1.4 mL/min of helium and the oven ran isothermally at 40 $^{\circ}\text{C}$ for 2.4 minutes, ramped to 80 $^{\circ}\text{C}$ at 40 $^{\circ}\text{C}/\text{min}$, and held at 80 $^{\circ}\text{C}$ for 0.25 minutes. The solvent delay lasted for 2.3 minutes and TCE and toluene eluted at 2.6 and 3.1 minutes, respectively. The inlet was set at 280 $^{\circ}\text{C}$ and the detector was set at 250 $^{\circ}\text{C}$.

4.6.3.1 Confidence interval. A 95% confidence interval was established for each sampling event for the inlet and outlet gas streams. The data from each calibration curve performed during the first phase of operation was pooled and the average response was related to the concentration-dependent standard deviation. Variance was not directly related to response in a linear fashion, but fit the collected data by normalizing with a function of the response. Equation 4-4 shows the model fitted standard deviation to

response relationship developed for the pooled data. The pooled standard deviation was compared with individual sample deviations and used to calculate a 95% confidence interval for each sampling event. Equation 4-5 was used to calculate the confidence intervals for each sampling event with the GC-FID. A similar relationship was established for the pooled GC-MS data and used to calculate confidence intervals.

$$\sigma_{\text{pooled}} = 3.6205 * \bar{X}^{0.6416} \quad (4-4)$$

$$\bar{X} \pm Z_{1-\frac{\alpha}{2}} * \frac{\sigma_{\text{pooled}}}{\sqrt{N}} \quad (4-5)$$

Where:

\bar{X} is the sample mean.

$Z_{1-\frac{\alpha}{2}}$ is the critical value of the standard normal distribution.

σ_{pooled} is the average normalized deviation from the standard curve times the sample response.

N is the sample size.

4.6.3.2 Method detection limit and limit of quantification. The method detection limit (MDL) and limit of quantification (LOQ) for the GC-FID and the GC-MS were established using the Environmental Protection Agency's (EPA) methods from 40 CFR Part 136. APPENDIX B, revision 1.11 for toluene and TCE. Four identical standards of toluene with a headspace concentration of 5.5 µg/L were analyzed in duplicate. For the GC-FID, equation 4-6 was used to calculate a MDL for toluene of less than 0.004 mg/L in the liquid phase with a signal to noise ratio of less than 10 but greater than 2.5. A set of four TCE samples, with duplicate injections, and a set of eight TCE samples with concentration of 9.9 µg/L, were analyzed to compare instrument variance

with variance in standard preparation. The instrument MDL for TCE was calculated to be less than 0.07 mg/L in the liquid phase and the MDL associated with standard preparation was estimated to be less than 0.08 mg/L in the liquid phase. The comparison showed that the inherent error associated with standard preparation is similar to the variance in typical machine operation. The variance from the two TCE MDLs were then used to calculate the pooled MDL (Equation 4-7), less than 0.03 mg/L in the liquid phase. The GC-FID LOQs for TCE and toluene were calculated using equation 4-8. The MDL and LC (4-6) values for the GC-MS were found using spiked 1.1 mg/L samples using the same (4-7) procedure outlined by the EPA. A summary of MDL and LOQ values can be found (4-8) in Table 4.2.

$$\text{MDL} = T_{(n-1)} * \sigma$$

$$\sigma_{pooled} = \left(\frac{6*\sigma_a^2 + 6*\sigma_b^2}{12} \right)^{1/2}$$

$$\text{LOQ} = 10 * \sigma$$

4.6.4. Other Analytical Methods. Chemical oxygen demand, pH, dissolved oxygen, water flowrate, and air flowrate were tracked during the entirety of the experiment.

4.6.4.1 pH. From July 2015 through August 2015 an Oakton pH 5+ Handheld Meter with pH probe was used to measure reservoir pH. The meter was calibrated using a two-point calibration method with standards of pH 4 and 7, from Fisher Science. The meter has an accuracy of 0.01 pH and a range from 0.00 – 14 pH. From September 2015 until the conclusion of the project, a Thermo Scientific Orion 3 Star Benchtop pH meter was used. The meter was calibrated using the same procedures as outlined above and had an accuracy of 0.002 pH over the range of 0.0 – 14. The pH meter from Thermo

Scientific was used to verify the results obtained using the Oakton pH meter, and was then used during the remainder of the experiment due to improved accuracy.

Table 4.2 MDL and LOQ values for GC-FID and GC-MS.

Chemical	GC-FID		GC-MS	
	MDL (mg/L)	LOQ (mg/L)	MDL (mg/L)	LOQ (mg/L)
Toluene	0.004	0.013	0.0015	0.0050
TCE	0.07	0.231	0.0010	0.0033
TCE (standard)	0.08	0.291	N/A	N/A
TCE (pooled)	0.03	0.096	N/A	N/A

4.6.4.2 Dissolved oxygen. From July 2015 through October of 2015 dissolved oxygen (DO) was measured in the reservoirs using a YSI model 68 dissolved oxygen probe and meter. The probe and meter have a range of 0 – 20 mg/L with a resolution of 0.01 mg/L and accuracy of 0.03 mg/L. The meter was calibrated daily according to local altitude and barometric pressure. A 0 mg/L DO standard and a saturated standard were used for a two-point calibration method. The saturated standard was prepared by bubbling compressed air in a flask filled with water for an extended period of time. The 0 mg/L standard was prepared by adding CoCl_2 and NaSO_2 to a flask containing 100 mL of water.

From October 2015 until the conclusion of the project, a YSI model 5000 dissolved oxygen probe and meter was used to check reservoir DO concentrations. The YSI 5000 probe had a propeller that increased the superficial velocity near the probe membrane that allowed for more precise readings. Very little difference was found between the measurements made with the 68 and 5000 model.

4.6.4.3 Chemical oxygen demand. During stimulated anaerobic operation of the membrane biological reactors the chemical oxygen demand (COD) was routinely measured to determine the rate of acetate degradation in each reactor. COD was measured using Method 8000 from HACH and the HACH DR 2000 Spectrophotometer. While holding a HACH COD digestion vial at a 45 degree angle, 2 mL of homogenized sample were pipetted into the vial. A blank was prepared in a similar fashion, but the homogenized sample was replaced by 2 mL of demineralized water. The vials were inverted several times to mix then placed in a 150 °C preheated COD digester and allowed to heat for 2 hours. After 2 hours the vials were allowed to cool for approximately 20 minutes, inverted to mix while still warm, and then placed in a rack to cool to room temperature. The blank was placed in the HACH DR 2000 Spectrophotometer and allowed to zero the instrument. The vials containing the sample were then placed in the instrument. The outside of each vial was cleaned with a damp and then dry cloth to remove any blemishes. COD standards were prepared using methods outlined in Method 8000 from HACH.

4.6.4.4 Water flowrate. The water flowrate was determined using a stopwatch and a graduated cylinder. The flow from the reactors was diverted to the graduated

cylinder (mL) for a period of time (min). The flowrate is determined by the measured volume over time, mL/min. The pump speed and pump fitting tightness were adjusted to get both reactors to a liquid-flowrate of 10 mL/min.

4.6.4.5 Air flowrate. A series of Cole-Parmer rotameters were used to control and measure the flowrate for various points in the system. A 3-point calibration curve was fitted for each rotameter using a TSI 4100 series flow meter and checked periodically during operation.

5. RESULTS AND DISCUSSION

In this experiment two hollow fiber membrane bioreactors (HFMR) were operated in parallel to treat gas phase VOCs for 215 days. A variety of loading rates and operating conditions were tested during that time. A loading curve for toluene degradation was established at low gas phase VOC concentrations. Batch experiments were conducted to test the ability of indigenous bacteria to treat toluene and TCE under aerobic and anaerobic conditions. Reductive dehalogenating bacteria (RDB) were subcultured and used to inoculate the reactors for the final phase of the project.

5.1. MASS TRANSFER ESTIMATES

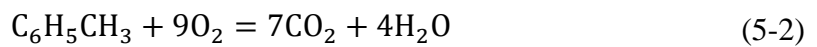
Before bioreactor start-up oxygen and toluene mass transfer was modeled to estimate steady-state dissolved oxygen concentration and to determine the necessary biochemical oxygen demand (BOD) needed to form anaerobic zones. The molar flux of oxygen and toluene were estimated using equation 2-1 and 2-2. The liquid phase mass transfer coefficient was estimated using an empirical correlation, equation 5-1. The gas phase mass transfer coefficient was assumed to be negligible for this situation and the biofilm mass transfer coefficient was assumed to be similar to the liquid phase. The membrane mass transfer coefficient was calculated using equation 2-2 and values from Table 5.1, adapted from England [75]. These calculations relied on a number of assumptions:

1. Steady state conditions in the reactor.
2. Diffusion dominates all mass transfer in the reactor.

3. The mass of oxygen in the gas phase did not decrease significantly due to the transfer through the membrane. This relationship was shown by relating the mass flowrate through the membrane to the mass flowrate in the air phase. It was found that less than 0.0009% of the mass of oxygen in the gas phase was lost through transfer into the reactor.
4. The mass of toluene in the gas phase does decrease over the length of the membrane. The total membrane mass transfer of toluene can be assumed by averaging inlet and outlet instantaneous flux over the length of the membrane. The inlet and outlet concentrations were estimated using values from England et al. [75] and then calibrated using system data.
5. Oxygen utilization in the reactor is stoichiometrically related to the toluene utilization, equation 5-2. Biomass is constant and toluene metabolism is used to maintain cellular function, this gives a conservative or “worst-case” scenario approximation.

A wide range of oxygen and toluene permeabilities in silicon rubber can be found in the literature. This wide range in measured and fitted values can make the estimated dissolved oxygen concentration vary from oxygen saturation (~8.5mg/L) to as low as 5.7 mg/L. This modeled DO is still well above the values measured during the 200+ day operation of the HFMRs. A corresponding BOD loading rate was estimated to account for the surplus oxygen mass transfer into the reactor.

$$\text{Sherwood Number} = \frac{k_1 d_o}{D_w} = 0.22 \text{Re}^{0.6} \text{Sc}^{0.33} = 0.22 \left(\frac{\rho d v_w}{\mu} \right)^{0.6} \left(\frac{\mu}{\rho D_w} \right)^{0.33} \quad (5-1)$$



Where:

k_l = Mass transfer coefficient in the liquid phase (cm s^{-1})

d_o = Fiber outer diameter (cm)

Re = Reynolds number (dimensionless)

Sc = Schmidt number (dimensionless)

μ = Shear viscosity ($\text{g cm}^{-1} \text{s}^{-1}$)

ρ = Density of water (g cm^{-3})

v_w = Water velocity (cm s^{-1})

D_w = Diffusion coefficient of substrate in water ($\text{cm}^2 \text{s}^{-1}$)

5.2. PHASE I: TOLUENE DEGRADATION AND LOADING

During phase I the reactors were seeded with toluene degrading bacteria from enriched activated sludge. Each HFMR was then operated for 110 days under a variety of toluene loading rates and GRTs and the resulting elimination capacities were measured. Dissolved oxygen, pH, biofilm thickness, and biofilm appearance were all recorded.

5.2.1. Biofilm Growth and Development. On July 22, 2015 both bioreactors were seeded with a culture that had been subcultured and grown on toluene exclusively for over 8 weeks. Initial biomass was collected from the southeast Rolla wastewater treatment plant in the spring of 2015. For the first several weeks, the microorganisms were fed a mixture of glucose and toluene. The headspace in the Erlenmeyer flask was tested routinely for toluene, and this was then used to determine the dosing schedule. After several weeks, significant biomass had accumulated and the sample was subcultured into a mineral media and exclusively given toluene as a substrate. After three weeks the community was again subcultured and dosed with toluene. A 1:100 mL/mL

Table 5.1 Mass transfer coefficients adapted from [75].

PARAMETER	Value
$P_{(\text{Oxygen in Silicone})}$	$1.63 \cdot 10^{-13} \text{ mol m}^{-1} \text{ s}^{-1} \text{ Pa}^{-1}$
$P_{(\text{Toluene in Silicone})} = D_m S$	$.000082\text{--}0.003 \text{ cm}^2 \text{ s}^{-1}$
$D_{(\text{Oxygen in Water})}$	$2.26 \cdot 10^{-5} \text{ cm}^2 \text{ s}^{-1}$
$D_{(\text{Oxygen in Air})}$	$0.219 \text{ cm}^2 \text{ s}^{-1}$
$D_{(\text{Toluene in Water})}$	$9 \cdot 10^{-6} \text{ cm}^2 \text{ s}^{-1}$
$D_{(\text{Toluene in Air})}$	$0.0849 \text{ cm}^2 \text{ s}^{-1}$
$H_{(\text{Oxygen } 20^\circ \text{ C})}$	$73,800 \text{ Pa m}^3 \text{ mol}^{-1}$
$\mu_{(\text{water } 20^\circ \text{ C})}$	$0.01002 \text{ g cm}^{-1} \text{ s}^{-1}$
$\mu_{\text{air } 20^\circ \text{ C}}$	$0.000182 \text{ g cm}^{-1} \text{ s}^{-1}$
$\rho_{\text{air } 20^\circ \text{ C}}$	$0.001205 \text{ g cm}^{-3}$
$\rho_{(\text{water } 20^\circ \text{ C})}$	998.2 kg m^{-3}
Length	21 cm
r_i	0.47625 cm
r_o	0.635 cm

ratio of seed to reactor volume was injected directly into the shell side of the reactors from the liquid sample port using biomass from this second subculture. After 24 hours, tiny clumps of white organisms were observed on the surface of the membranes and after 5 days a thin layer of biofilm had accumulated on both reactors. On day 6, suspended clumps of organisms were found in the liquid phase of the shell and reservoir of each reactor. The biofilm in both reactors started to have sparse green clusters, and by day 21 the entire biofilm had changed to a greenish-brown color. Pictures of biofilm development can be found in the A.

Measuring biofilm thickness is often a difficult task that either requires expensive cameras and microscopes or requires sacrificing the biofilm. This project used a projector to allow for *in situ* measuring of the biofilm by projecting light through the glass modules

and magnifying the membrane and surrounding biofilm on a nearby screen. This method was adopted from techniques outlined by Freitas dos Santos and Livingston [81]. Biofilm thickness was measured on two sides of the reactor at 12 equidistant lengths covering approximately two-fifths of the reactor length, Figure 5.1. For the first several days the biofilm consisted of heterogeneous clumps that made measuring impossible, but by day 7 biofilm thickness could be measured for the length of the membrane. The left and right thicknesses were then combined and used to estimate the overall area of biofilm at heights along the membrane. The area was estimated by assuming a circular biofilm offset from the membrane. The volume was then calculated by summing each area over a length of membrane, Figure 5.2. During the growth phase the biofilm thickness and volume seemed to plateau on day 10 and then fluctuate slightly until day 23.

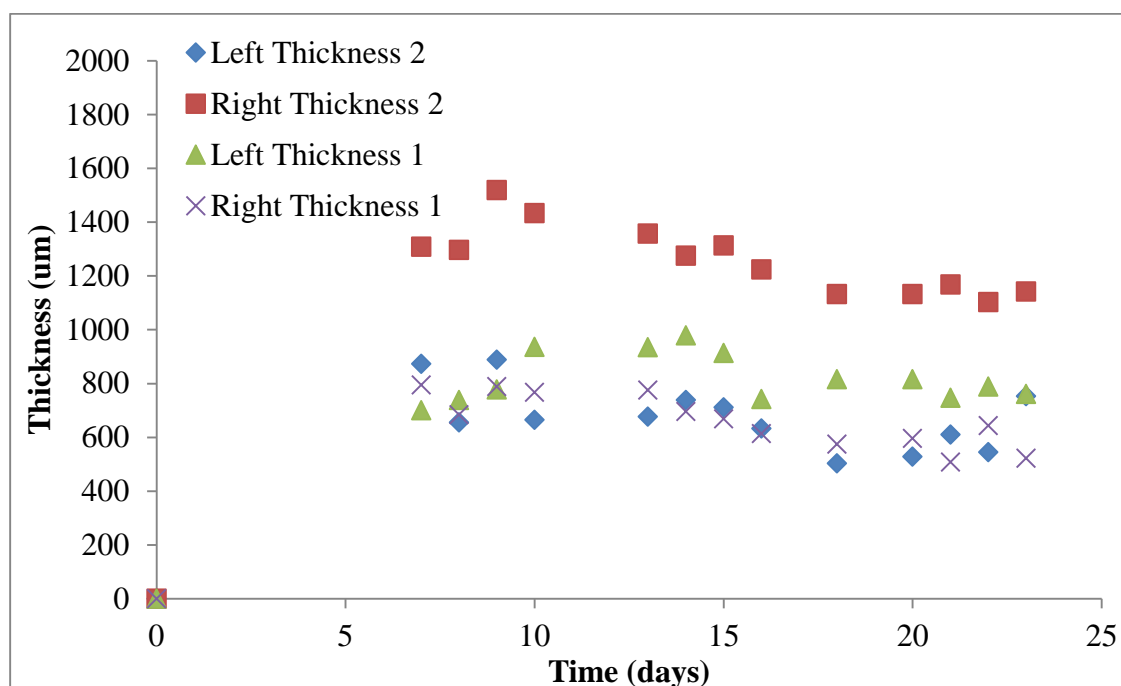


Figure 5.1 Measured biofilm thickness in the growth phase.

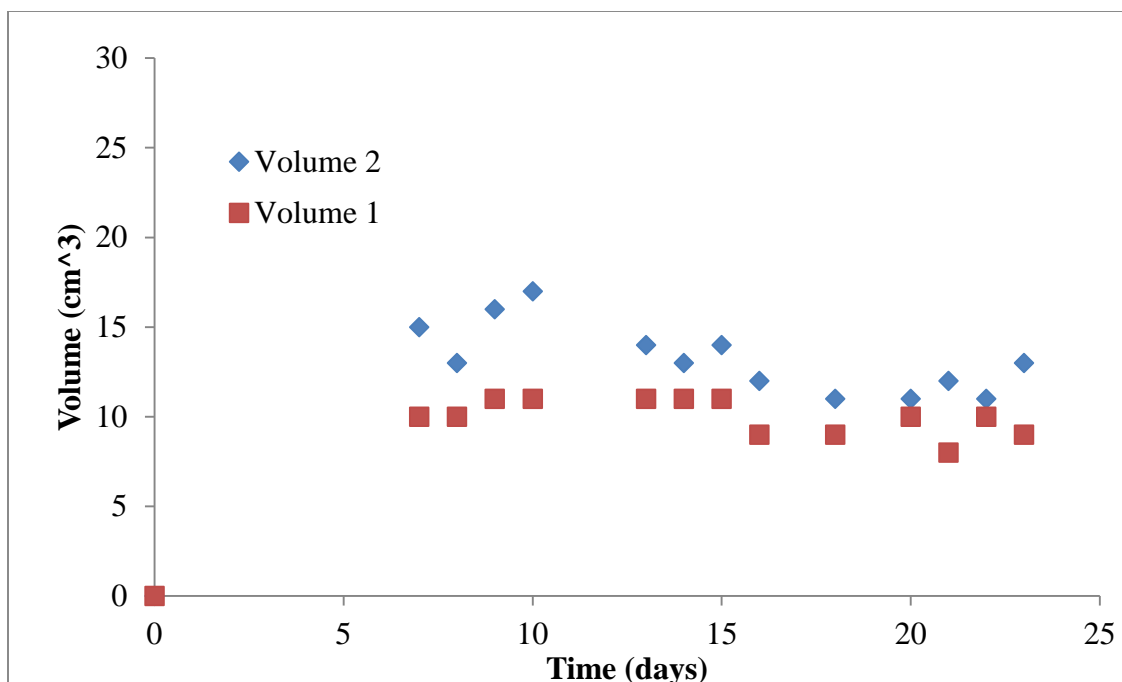


Figure 5.2 Estimated biofilm volume during growth phase.

Prior to inoculation, the liquid mineral media had reached equilibrium with the gas phase toluene stream; this caused the liquid phase concentration in the reactors to be 64-67 mg/m³, which was proportionate to the estimates from Henry's law constant. As the biofilm and suspended microorganisms developed, a steady decline in liquid phase toluene was observed, Figure 5.3. During the growth phase, the liquid concentration of toluene seemed to be independent of the membrane loading rate, but an increase in observed suspended organisms did correlate to the decrease in total mass of soluble toluene.

The pH for each system was measured routinely from the reservoir during the entirety of the experiment. As the biofilm and suspended growth developed, a constant decline in pH was observed, Figure 5.4. The slow pH drop was initially attributed to the

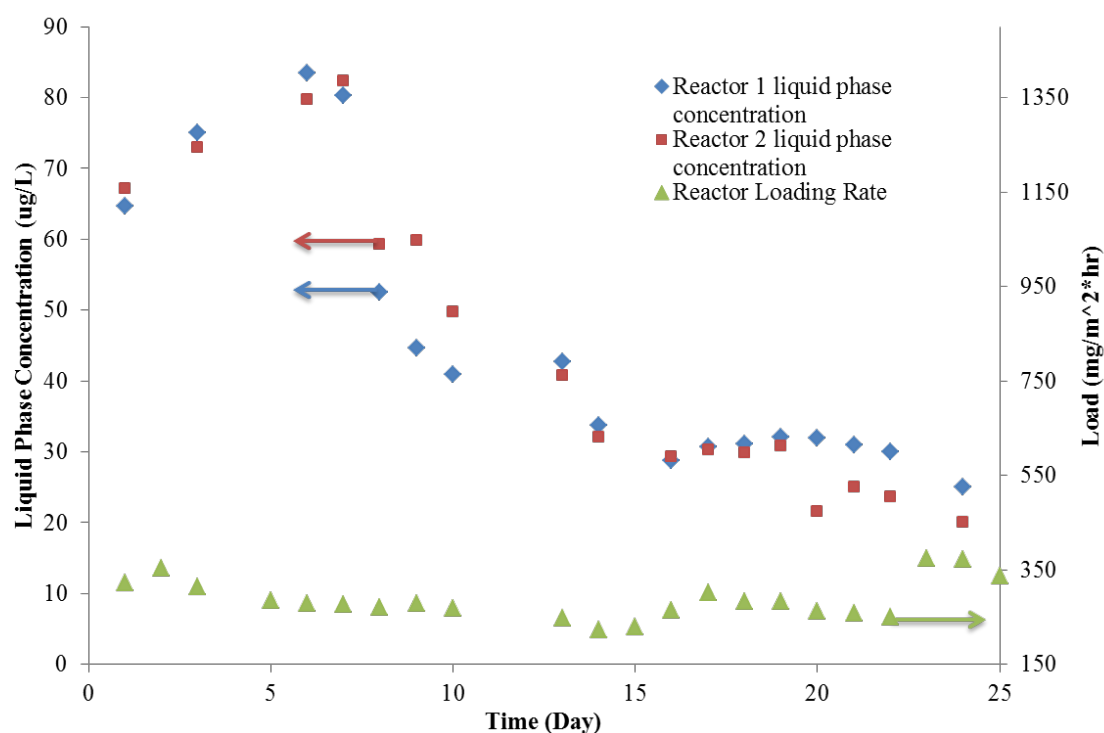


Figure 5.3 Reactor loading rates and liquid phase toluene concentration during the growth period.

production of CO₂ through toluene metabolism. The mineral media had been designed to have buffering capacity, so the steady decline in pH was surprising. During the growth phase the rate of acidification was fairly slow, with pH dropping from 6.64 to approximately 5.7 in 23 days. The DO in both reactors was measured as less than 1 mg/L which is below a quantifiable level for most DO probes and meters. The estimated DO was significantly higher than the observed DO, which was likely caused by a reduction in mass transfer due to variations in silicone tubing production. The steady decline in pH and the low measured DO led to the assumption of partial anaerobic metabolism leading to the production of fatty acids.

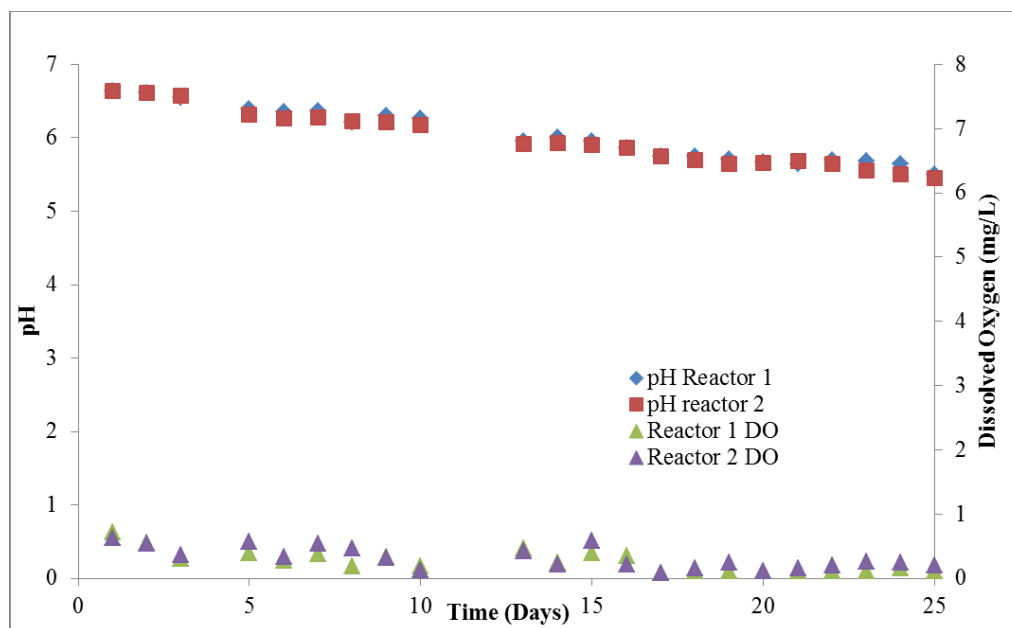


Figure 5.4 Dissolved oxygen concentration and pH during growth period.

During the growth period the gas phase inlet and outlet concentrations were tracked daily for both reactors, Figure 5.5. During the first 8 days, little to no removal could be attributed to microbial degradation which correlated with biomass development. During the growth period the average toluene air concentration was 195 mg/m^3 (LCL 183 mg/m^3 , UCL 207 mg/m^3) and the final outlet concentrations in reactors 1 and 2 were 140 mg/m^3 and 145 mg/m^3 , respectively. After 23 days, the elimination capacity (EC) of each reactor had stabilized to approximately $50 \text{ mg m}^{-2} \text{ hr}^{-1}$ and $45 \text{ mg m}^{-2} \text{ hr}^{-1}$ for reactors one and two, respectively. Very small variances in EC and biomass growth for several sampling events lead to an assumption of quasi steady state removal in each reactor.

5.2.2. Steady-State Toluene Removal. From day 23 through day 110 the toluene load and GRT were varied to determine optimal operating conditions and to develop a

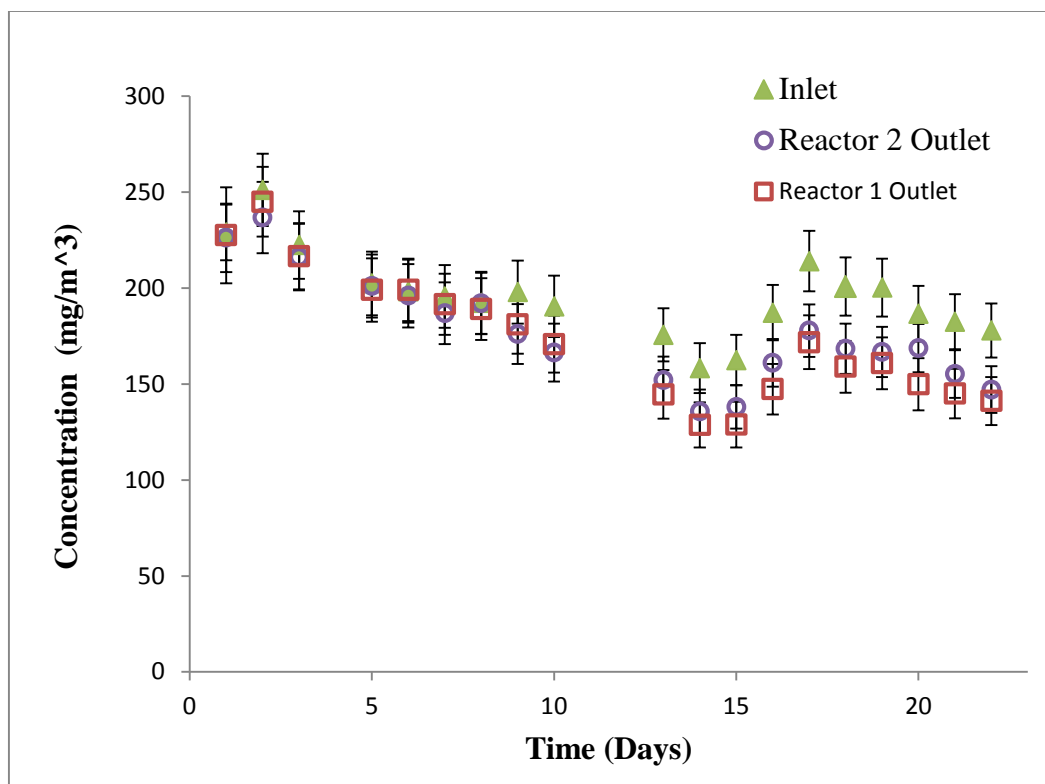


Figure 5.5 Reactor inlet and outlet toluene gas concentrations in the growth period.

loading curve, Figure 5.6. For each GRT examined, multiple loading rates were tested to compare the degradation potential with varying driving forces. At each loading rate several sampling events, over a minimum of 48 hours, were conducted to assure quasi-steady state. After this steady-state was achieved, the load or GRT could be adjusted. The pH continued to decrease steadily and the biofilm thickness was measured until excess growth made it impossible. The excess growth prevented the light from penetrating the modules, so no measurements could be made on the nearby screen.

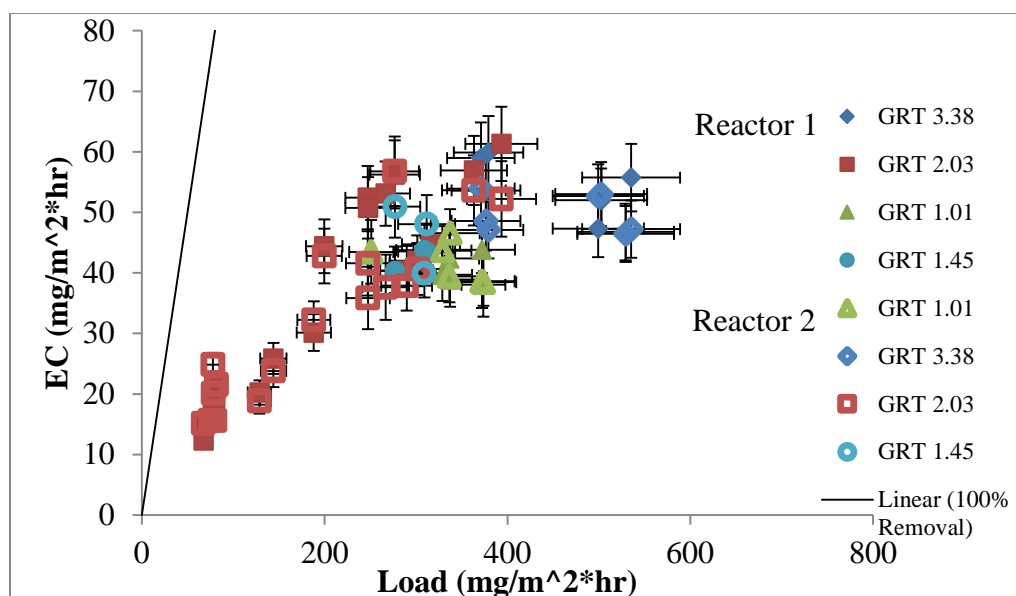


Figure 5.6 Toluene elimination capacity in reactor 1 and 2. GRT in seconds.

The GRT seemed to have some effect on each reactor's EC over the small range tested in this experiment. When the gas flow was increased to 1 LPM and the GRT was reduced to 1.01 seconds, an approximately 30% reduced in the EC was observed compared to the EC for a GRT of 2.03 seconds. The reduction in EC at lower GRTs is likely related to a reduction in the concentration gradient, driving force, at similar same loading rates; a lower GRT is a higher flow rate and thus the concentration is lower at the same mass loading rate. Little to no increase in removal was observed when the gas flowrate was reduced to 0.3 LPM and the GRT increased to 3.38 seconds, this resulted in a gas flowrate of 0.5 LPM to be used for the duration of the experiment.

Under very low toluene loading rates, $0\text{--}200 \text{ mg m}^{-2} \text{ hr}^{-1}$, a significant reduction in removal was observed in both reactors. The EC of each reactor seemed to peak between $50\text{--}60 \text{ mg m}^{-2} \text{ hr}^{-1}$ for loading rates between $200\text{ and }400 \text{ mg m}^{-2} \text{ hr}^{-1}$. These observations

lead to a hypothesis that the reactors were operating under mass transfer limiting conditions from 0-300 mg m⁻² hr⁻¹ but transitioned to kinetic limitation above 300 mg m⁻² hr⁻¹. In the literature, ECs were reported an order of magnitude higher than values observed in this study, so it seemed unlikely the reactors were kinetically limited. [25-27, 75]. It is more plausible that the reactors were mass transfer limited with low chemical driving force at these low loading rates.

During the entirety of the toluene degradation phase (phase I) the DO in both reactors was never measured above 1 mg/L, Figure 5.7. The DO was checked with multiple meters and calibrations were performed using anoxic and saturated solutions. From day 48 through 74 more noise in DO measurements was observed. This was likely due to the addition of small amounts of liquid phase into the reservoirs to balance out liquid losses. On day 37 a sodium bicarbonate solution was added in an attempt to increase the buffer capacity of the liquid phase. From day 45-109, no attempts to control pH were implemented and all increases in pH are due to replacing losses from the liquid phase with fresh media. During phase I, a steady decrease in pH was measured from 6.64 to approximately 3.8 in each reactor. It was theorized that the drop in pH was caused by anaerobic metabolism and by the production of fatty acids.

No significant correlation between pH and EC was observed in either reactor during the duration of the experiment, Figure 5.8. Over a pH range of 6.6-3.8, no pH dependent fluctuation in EC was observed, but this is a relatively small range pH range. At a pH below 3 the reactors would likely experience a significant decline in performance due to increased hydrogen concentration gradients and potential toxic effects on the

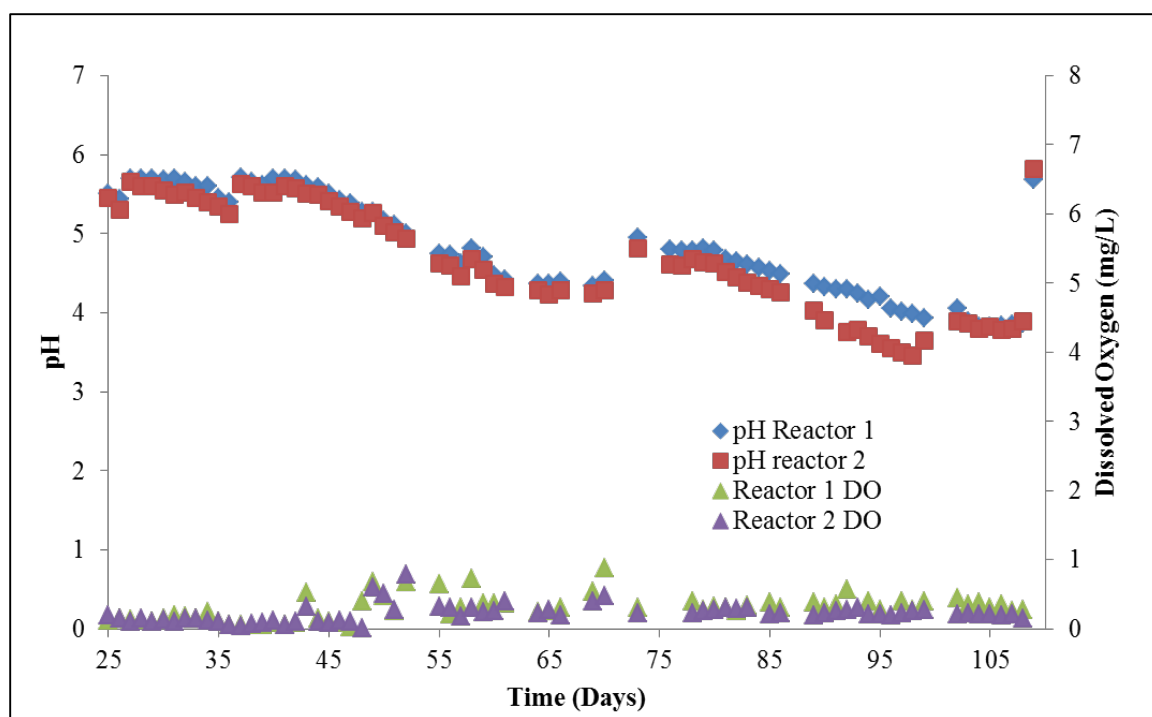


Figure 5.7 Dissolved oxygen concentration and pH during phase I.

microorganisms. At a pH of approximately 3.8 the reservoir was drained and replaced with fresh mineral media which raised the reactor pH to 5.9

For the first 76 days the biofilm thickness in reactor two was measured and used to estimate biofilm volume, Figure 5.9. On day 76 the suspended organisms in the liquid phase and biofilm became too thick to allow sufficient light through the system to measure the biofilm. A large increase in biofilm was observed from day 27- 40 which was likely caused by the addition of concentrated phosphate buffer solution. That buffer solution was added on day 26 to try and control the decrease in pH. A large increase in biomass was observed which means the reactor was likely nutrient limited. Around day 40 the biofilm thickness and volume seems to have plateaued again.

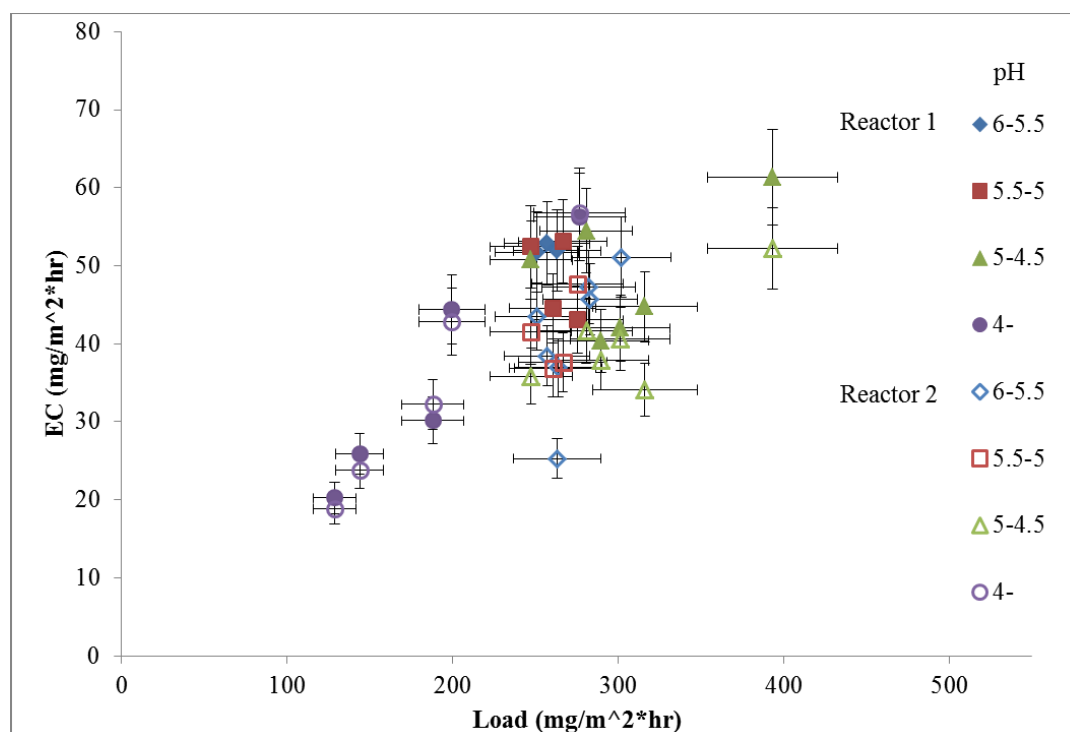


Figure 5.8 Elimination capacity and pH relationship in phase I.

After 28 days of operation the biofilm shifted in color from green to black and after 47 days the outer biofilm started to turn yellow. From day 69-110 the biofilm was a relatively homogeneous black color. The formation of metallic sulfides by sulfate-reducing bacteria could potentially explain the shifts in biofilm color to black. Under anaerobic conditions, sulfate-reducing bacteria form H_2S from the SO_4 species in the mineral media. The H_2S can dissociate and form metallic sulfides with the macro and micro metals in the system, leading to a dark brown or black color. The yellow or orange color could be due to speciation of iron or the presence of methanotrophic bacteria [82]. On day 110, one-third of the liquid media was replaced with fresh mineral media which led to a dramatic increase in biomass in the system. The used liquid media was separated

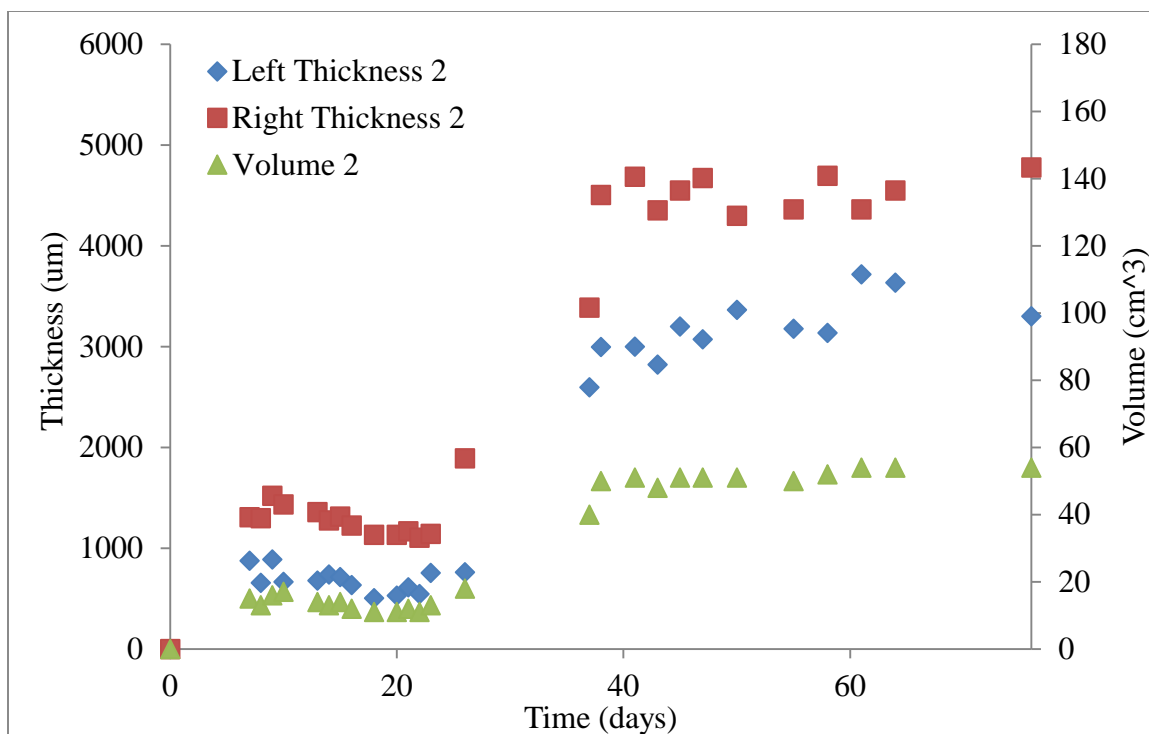


Figure 5.9 Reactor two biofilm thickness and volume.

and used to test toluene degradation, co-metabolism, and reductive dehalogenation of indigenous bacteria in a batch experiment.

5.2.3. Indigenous Batch Experiments. Before TCE was added to the gas phase in the HFMRs a set of batch experiments were conducted to test the ability of the indigenous bacteria to degrade toluene and TCE. The liquid from both reservoirs was collected and gently homogenized in an attempt to standardize each bottle and each test was done in duplicate. Two 260-mL bottles were each filled with 50 mL of distilled water and approximately 7 μg of toluene to act as controls. Four 260-mL bottles were filled with 50 mL of the aerated liquid phase from the reactors. All four of the bottles were then dosed with 7 μg of toluene and two of those were also dosed with approximately 50 μg of

TCE. The last two bottles were filled with 50 mL of the liquid phase from the reactors which had been deoxygenated under a 99.9 % pure stream of N_2 for approximately 45 minutes. The deoxygenated liquid was then dosed to 30 mM of acetate and 50 μ g of TCE. All eight bottles were then placed on an orbital shaker at 250 rpm for 72 hours. The headspace of each bottle was analyzed routinely using the GC-MS and the total mass of each compound was estimated using the temperature dependent Henry's law constant, Figure 5.10.

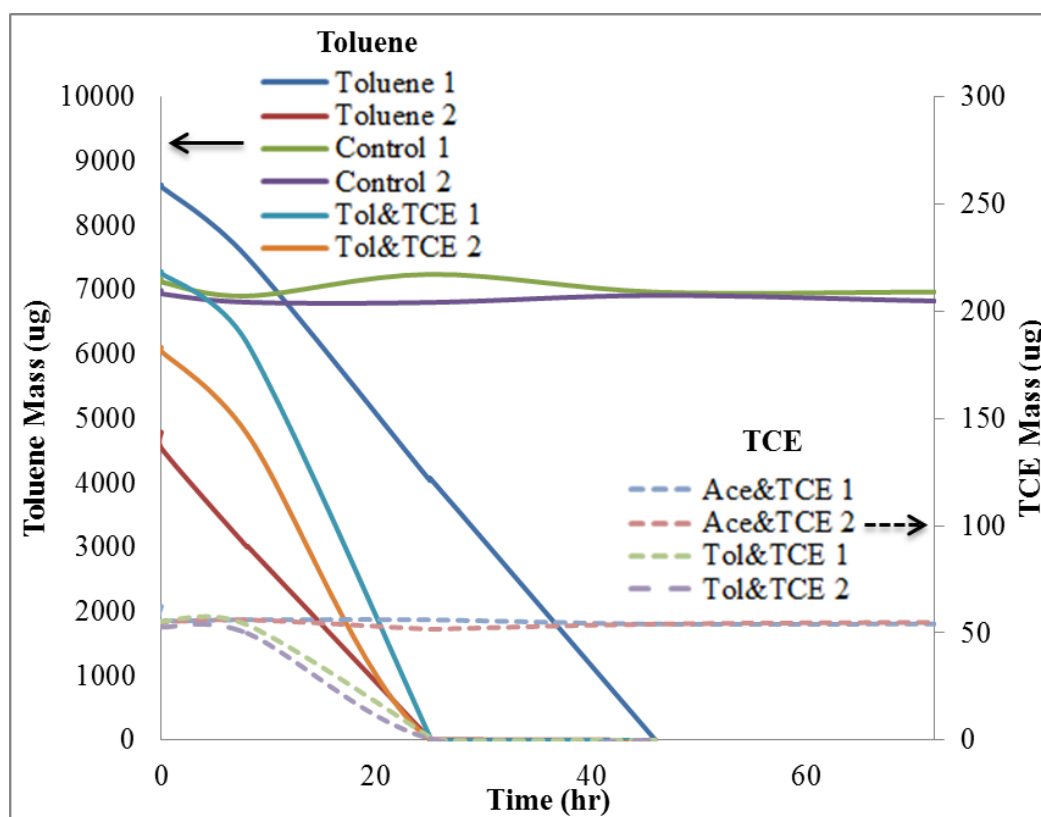


Figure 5.10 Aerobic and anaerobic batch experiments with indigenous bioreactor bacteria.

The toluene controls varied over the course of the experiment but the starting mass and ending mass measurements were less than 1% apart. The large fluctuation observed near the end of the first day is likely due to a shift in temperature or caused by residual toluene in the syringe prior to injection in the GC. The mass of toluene in the headspace of these experiments made traditional syringe cleaning insufficient to prevent carryover. In the toluene degradation experiments and co-metabolism experiments the toluene mass dropped slowly during the initial 8 hours, then more quickly until toluene was no longer detected. Toluene 1 had a much slower rate of degradation than toluene 2, and took 16 hours longer to achieve complete removal. Prior to the first round of injections (2.5 hours after dosing), toluene 2 mass had already dropped to 64% of the mass of the controls. This result could be explained by losses from the bottle but the negligible loss in mass from the controls makes it unlikely. The initial loss and more rapid rate of degradation in toluene 2 could be caused by a higher mass of more active bacteria than in toluene 1. The toluene and TCE masses in the co-metabolism bottles were near the MDL level after 24 hours but no loss in TCE was observed within the first 8 hours. This lag in TCE removal is likely linked to enzymatic preference and by the lack of mono or dioxygenase activity within the first several hours of the experiment. TCE and toluene were undetectable after 48 hours in all aerobic tests. During the anaerobic TCE and acetate experiments no quantifiable TCE removal was observed. These results were not surprising because the initial seed lacked exposure to chlorinated hydrocarbons and likely lacked reductive dehalogenating bacteria (RDB). These batch experiments showed that the indigenous bacteria in each HFMR were capable of toluene and TCE co-metabolism but were likely incapable of anaerobic reductive dehalogenation.

5.3. PHASE II: CO-METABOLISM OF TOLUENE AND TCE

On day 110 of operation, November 9, 2015, TCE was added to the air phase in both reactors at a low loading rate. Phase II investigated the possibility of co-metabolism of TCE in silicone HFMRs. Excess biomass made measuring the biofilm impossible but the biofilm thickness and color seemed to remain constant during phase II of the experiment. The DO concentration remained below 1 mg/L and the pH was controlled using NaOH.

During the entirety of phase II operation no TCE removal above the mass closure rate was observed in either reactor, Figure 5-11. Low TCE removal was observed in the first week, but this was likely due to accumulation in the system (water, tubing, rubber stoppers.) On day 10 of phase II aeration was added to the reservoir of reactor two to investigate if oxygen limitations were limiting toluene degradation and TCE co-metabolism. No increase in toluene or TCE removal was observed in reactor two after the addition of aeration, Figure 5.12. From day twenty to the conclusion of phase II the toluene load was dramatically increased in an attempt to facilitate co-metabolism of TCE. The molar toluene to TCE ratio was raised from 4:1 to 6:1, which aligned with molar ratios used in literature [21, 41]. The increase in substrate molar ratio had no observable effect on toluene or TCE elimination capacity. The measured TCE-EC was never above 5 mg m⁻² hr⁻¹, which is below the abiotic loss measured prior to biotic operation.

Starting November 13th the pH was controlled using 1 M NaOH to a small range of 7-7.5. This was done to test the effect of pH on TCE and toluene removal and to prepare for the addition of RDBs. From day 70-136 both biofilms were a relatively homogeneous black color, but on day 137, reactor one started to shift to a yellow color.

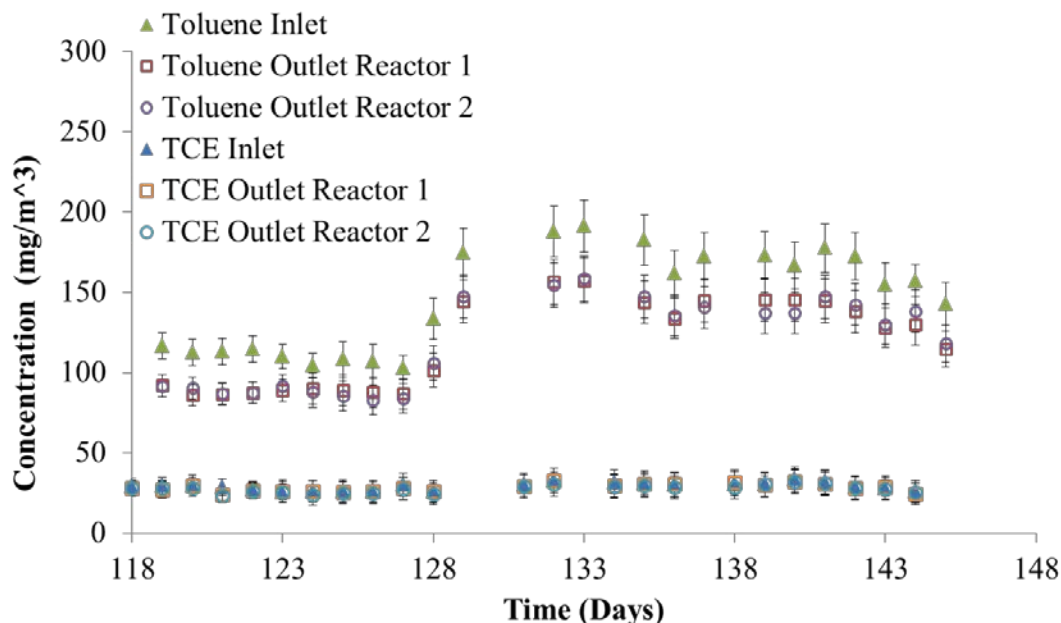


Figure 5.11 Toluene and TCE inlet and outlet concentrations in phase II.

By day 139 that reactor had shifted to a uniform golden-brown color, Figure 5.13. The shift in color was prior to the addition of acetate and 30 days after TCE was added to the system. Reactor two maintained a black, fluffy biofilm during the aeration portion of the experiment. On day 148, the aeration was removed from the system and by day 152 both reactors were the same fluffy, golden-brown color, Figure 5.14.

On December 7th sodium acetate (55 mg/L/day) was added to the liquid phase in order to stimulate RDB and to provide an additional source of BOD. Controlling the pH and the addition of acetate to the system had no observable effect on the elimination capacity of either reactor, Figure 5.15. It was surprising that the addition of acetate in the liquid phase didn't have an inhibitory effect on toluene degradation. The acetate loading was related to TCE load and was kept to a minimum to try to limit negative interactions.

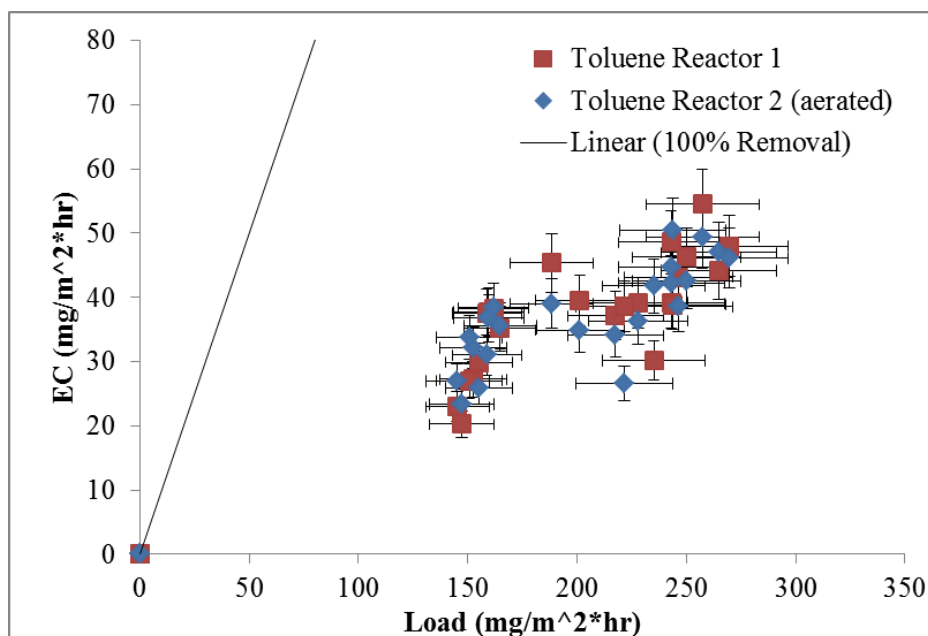


Figure 5.12 Toluene elimination capacity in reactors one and two during phase II.



Figure 5.13 Reactor two (aerated) (left) and reactor one (right) (12/6/15).



Figure 5.14 Reactor two (left) Reactor one (right) (12/20/15).

The COD of each reactor was checked regularly and no accumulation of COD (BOD) was observed. The acetate likely was consumed before diffusing into biofilm zones near the membrane where the majority of toluene degradation occurred.

Phase II of this experiment attempted to facilitate co-metabolism of TCE in parallel silicone HFMRs with a variety of operating parameters. No TCE degradation was observed during the entirety of phase II. Adjusting the substrate molar ratio, pH, DO concentration, and the addition of BOD all failed to affect the toluene or TCE removal in these reactors. In December of 2015 two communities of RDBs were obtained and subcultured. Dehalogenation was confirmed for both cultures and then samples were used to inoculate both reactors.

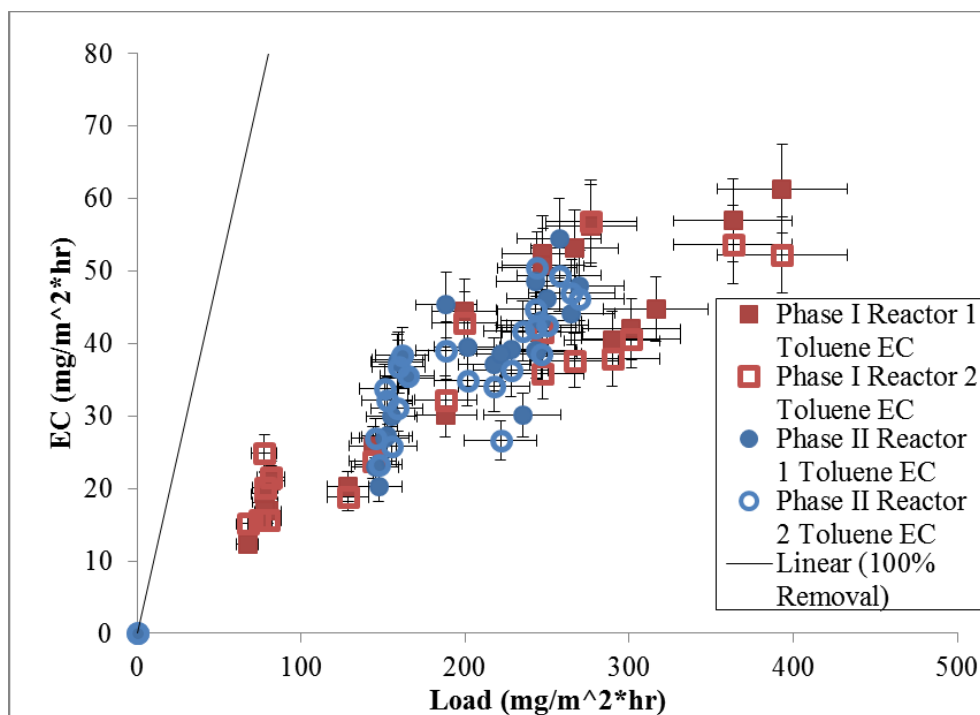


Figure 5.15 Phase I and II toluene elimination capacities in both reactors.

5.4. PHASE III: ADDITION OF REDUCTIVE DEHALOGENATING BACTERIA

A large objective of this experiment was to investigate the potential for anaerobic reductive dehalogenation to degrade chlorinated solvents from an aerobic gas phase. To achieve this goal, particularly after no TCE removal in phase II, RDB bacteria needed to be added to the HFMRs and sufficient electron donors needed to be present. Phase III included the sub-culturing of established RDB communities, inoculation, and the long-term operation of both HFMRs.

5.4.1. Subculture Development. In December 2015 the two RDB communities were subcultured, biomass was developed, and dehalogenation was investigated.

Subcultures were established using a 1:100 ratio of seed to media in 255-mL amber glass bottles with Mininert[®] caps. The anaerobic mineral media was produced following established techniques outlined in Löffler et al. [78]. Each bottle was filled with 100 mL of anaerobic media inside of an anaerobic glovebag. The headspace of each bottle was adjusted to approximately 5% H₂ and acetate was added to a concentration of 30 mM. Each bottle was then dosed with 50 µg of tetrachloroethylene (PCE) and placed on an orbital shaker at 150 RPM. The headspace was routinely analyzed for chlorinated solvents to look for evidence of dehalogenation. After 48 hours PCE and TCE levels had fallen below the MDL and fragments associated with ethene were measured. The anaerobic media was then replenished with acetate to a concentration of 100 mM and the headspace was adjusted with H₂. Each bottle was then dosed with 100 µg of PCE and placed on an orbital shaker. The headspace was routinely analyzed and the liquid phase was checked for biomass development. After all chlorinated solvents had been degraded and sufficient biomass was observed, 7 mL of each subculture was injected into the liquid port of each reactor. The aeration had been shut off previously and the liquid phase in each reactor was anaerobic.

5.4.2. Operation. No TCE removal above the mass closure estimates was observed after inoculating the reactors with RDBs, Figure 5.16. Reductive dehalogenating bacteria are typically slow growing, so the experiment was operated for an extended period of time to allow for growth [49, 78]. On day 45 of phase III, yeast was added to the liquid phase to act as a source of vitamin B12, which is a required micronutrient for most dehalogenate enzymes[6, 78]. The percent removal of TCE varied

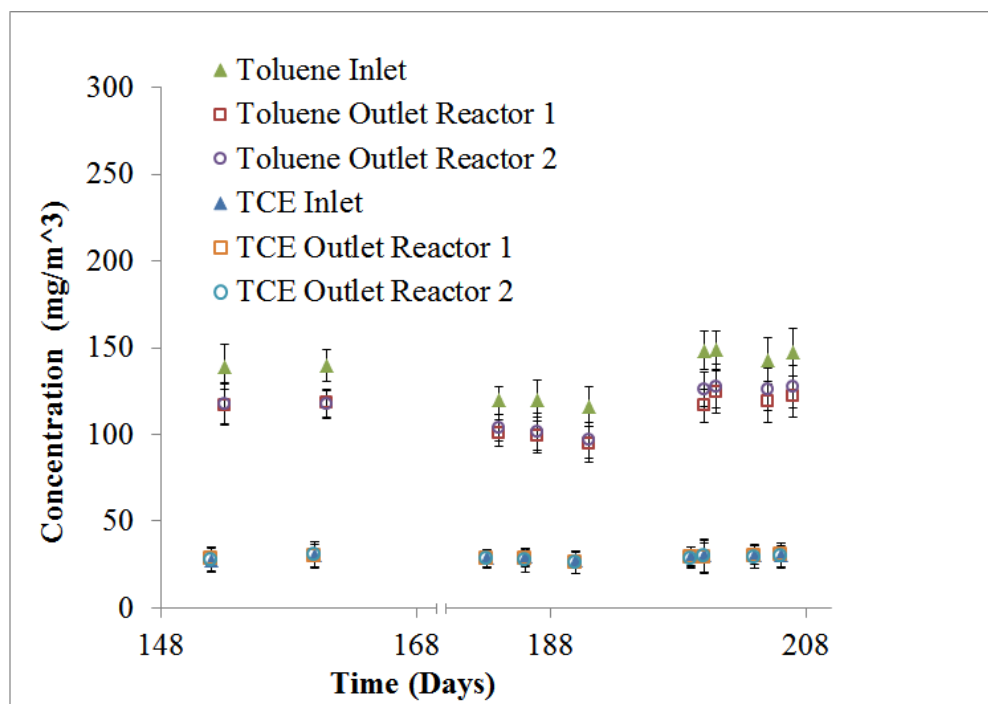


Figure 5.16 Toluene and TCE inlet and outlet concentrations in phase III.

from -3 to 4 %, and the calculated EC was below $5 \text{ mg m}^{-2} \text{ hr}^{-1}$. These values are all below the mass closure estimates conducted during abiotic operation.

During phase III operation, a declining trend in toluene EC was observed, Figure 5.17. The average removal at the same loading rate saw a 10-50% reduction in EC during the final phase of this experiment. There are several theories to explain this decline in toluene removal: (1) a reduction in mass transfer, (2) inhibition caused by acetate or intermediate metabolism, and (3) aging of the biofilm.

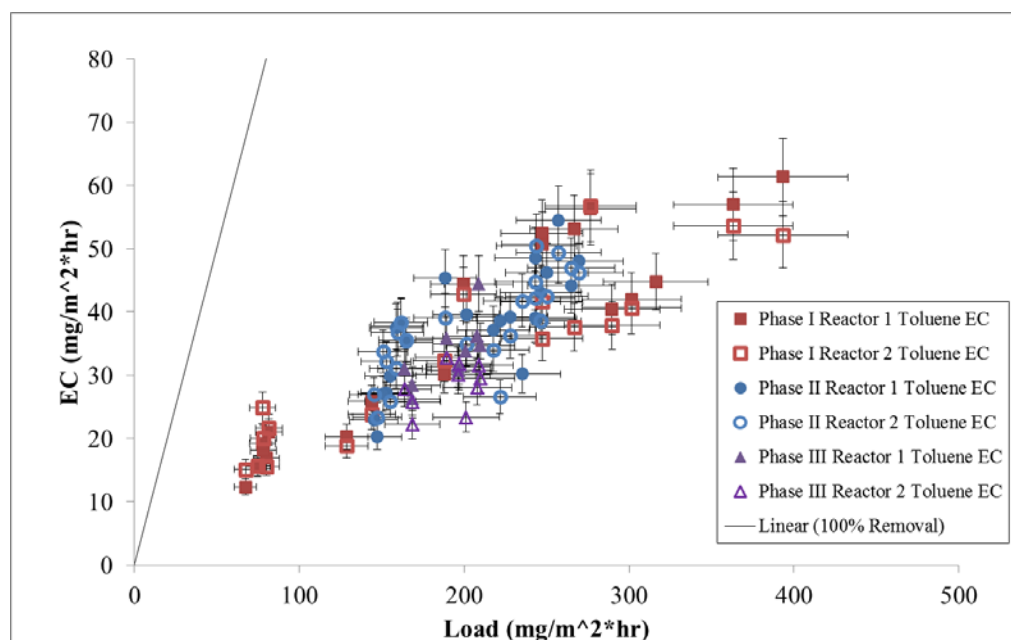


Figure 5.17 Toluene elimination capacity in phase I, II, and III.

- (1) From December 22-26th both membranes stretched out inside of the reactors, Figure 5.18. The tensile change in each membrane could have reduced the mass transfer in the system and could account for the decrease in toluene removal. The stretched membranes have significantly more contact with the wall of the reactor, which could negatively impact the biofilm.
- (2) Shortly after the start of phase III the pH stabilized and addition of NaOH was ceased. Two weeks after the addition of RDB, the pH began to steadily increase from 7.2 to 7.8, Figure 5.19. The pH was then adjusted using 1 N HCL to stay within the recommended pH window for RDBs [48, 78]. The increase in pH could be related to an inhibitory metabolism of some intermediate.



Figure 5.18 Membranes before and after membrane stretching.

- (3) The reduction in toluene removal could be related to the aging of the biofilm and the buildup of toxins or inactive mass. Over the course of the experiment several shifts in mass and color have occurred that could be used to indicate shifts in population and dominate species.

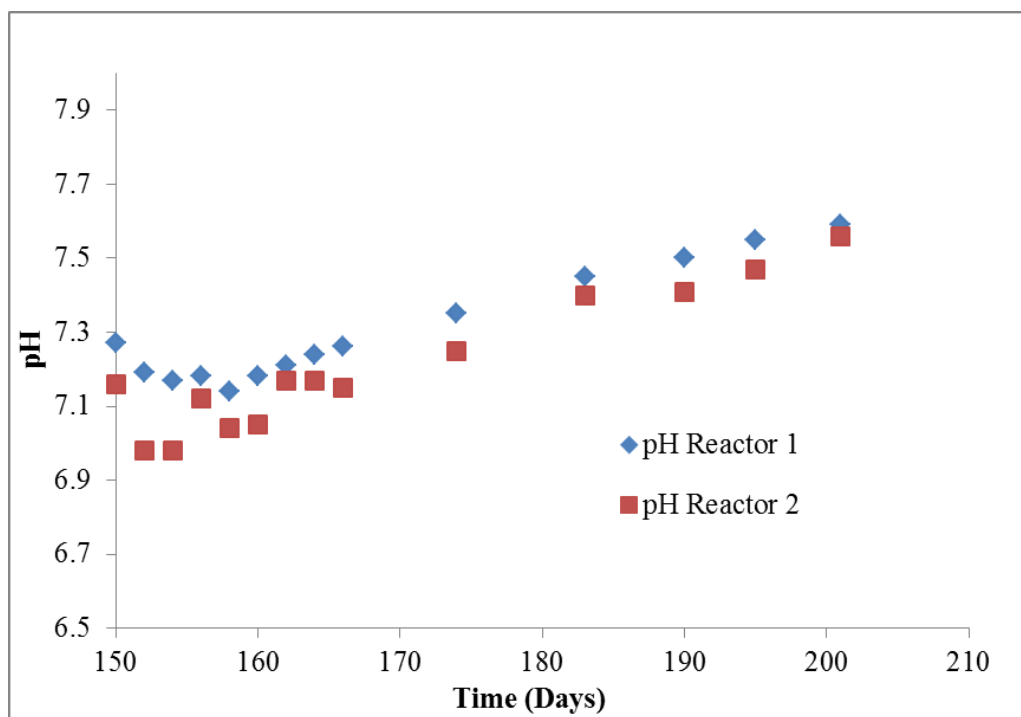


Figure 5.19 Phase III pH shift over time.

6. CONCLUSION AND RECOMMENDATIONS

Experiments using two HFMRs in parallel were conducted over a variety of operating conditions for a total of 215 days to investigate the use of silicone HFMR to treat VOCs. In that time, toluene degradation, TCE co-metabolism, and TCE dehalogenation were tested using batch experiments and quasi-steady state HFMR operation. The silicone HFMRs were able to remove toluene over a range of loading conditions, but were unable to degrade TCE during operation.

6.1. OBJECTIVE 1: TOLUENE LOAD AND ELIMINATION CAPACITY

The first objective was to operate two toluene degrading silicone HFMRs over a range of loading rates and operating conditions to determine optimal operating parameters and to develop a loading-elimination capacity curve. During fall 2015, both HFMRs were used to treat gas phase toluene over GRTs ranging from 1-3 seconds and loading rates ranging from 50-450 mg m⁻² hr⁻¹. The collected data was used to construct a toluene loading-elimination capacity curve, Figure 5.6. Elimination capacities were also related to the shift in pH but no correlation was observed. The biofilm thickness was measured and used to calculate a biofilm volume during the first phase of the experiment.

The range of loading tested in this experiment are very low and much higher loads should be tested in the future to construct a larger curve. The pH values tested in this phase of the experiment ranged from 6.4-3.8 and it's possible a decline in removal could be observed outside of this range. The toluene degradation phase lasted for 110 days which could demonstrate long-term removal, but around day 155 the membranes began to stretch out and a decline in removal was observed. Many variables were changed from

day 110 to 155 so it cannot be concluded that toluene degradation caused this issue. A long-term toluene degradation experiment to estimate membrane lifetime would be useful to establish membrane lifespan.

6.2. OBJECTIVE 2: AEROBIC TCE CO-METABOLISM

In November 2015 TCE was added to the gas phase at a low loading rate and co-metabolism was investigated for 40 days. In the literature, the addition of TCE to the system nearly always resulted in a reduction of toluene removal, but no decline was observed in this experiment, Figure 5-12. No TCE removal was observed in the first 20 days at a molar ratio of 4:1 toluene to TCE, so the ratio was adjusted to 6:1 and operated for an additional 20 days. During the entirety of this phase no TCE removal was measured above the rate of mass closure.

During this experiment very low loading rates and only two molar ratios of toluene and TCE were tested. Future projects should investigate a wider range of loading rates, including significantly higher toluene rates. The molar ratios of toluene to TCE were lower than many investigated in the literature and rates as high as 50:1 should be tested in silicone HFMRs.

6.3. OBJECTIVE 3: AERATION

Mass transfer estimates and previous experiments led to predictions of oxygen limiting conditions in the liquid phase and the biofilm. The addition of aeration to the liquid phase in the reservoir was investigated to overcome oxygen limitations and to attempt to increase oxygenase activity. On day 10 of phase II (day 121), aeration was added to the reservoir of reactor two and elimination capacities were measured for 30

days, Figure 5.12. The DO concentration in reactor two quickly increased to saturation, but no effect on TCE or toluene removal was observed. During the aeration phase the pH stopped gradually dropping and a large increase in suspended biomass was observed. During the aeration phase, clogging of tubing became an issue and excess biomass was removed several times to prevent complete system failure.

Aeration might be more beneficial under significantly higher VOC loading rates. Future research should investigate the addition of aeration under kinetic limiting conditions rather than mass transfer limited conditions to see if aeration can significantly increase the kinetic limitation. Future projects should also consider using the nutrient media C/N/P concentrations and ratios to control biomass in the membrane and to prevent clogging.

6.4. OBJECTIVE 4: BATCH TCE AND TOLUENE DEGRADATION

Prior to phase II or III operation it was necessary to test the ability of the indigenous microorganisms in the bioreactors to degrade toluene and TCE both aerobically and anaerobically. Approximately 300 mL of the liquid phase from each reactor was collected and homogenized to use in batch experiments. Duplicate experiments were run to test toluene degradation, TCE co-metabolism, and anaerobic reductive dehalogenation against controls. Complete removal of toluene and TCE was observed under aerobic conditions but no TCE removal was measured under anaerobic conditions. The batch results were unsurprising, but it seemed to contradict the lack of TCE removal measured in the reactors. TCE removal in the batch experiments was observed after several hours and the operating conditions in the HFMRs were likely not optimal to mimic the removal measured in the batch experiments.

In future batch experiments, the removal and biomass could be more closely monitored to fit kinetic parameters for modeling. Several batch experiments could be performed over the course of HFMR operation to measure kinetic shifts in bioreactor bacteria composition. More batch experiments at a variety of substrate molar ratios should be performed to explain HFMR results and to find optimal operating conditions.

6.5. OBJECTIVE 5: ANAEROBIC TCE DEGRADATION

During existing operating conditions, the viability of facilitating reductive dehalogenation in the existing anaerobic zones in the biofilm was investigated prior to the addition of established RDBs or acetate. Even though mass transfer estimates predicted DO concentrations of 5.7-8.5 mg/L, the measured DO never surpassed 0.7 mg/L. This means it was plausible that anaerobic conditions existed within the bioreactor and biofilm that could allow for the development of RDBs.

Future experiments should use additional sensors to better measure redox potential in the reactor and in the biofilm. Microsensors could be used to measure oxygen gradients in μm increments within the biofilm, but significant modifications to reactor configuration would be required.

6.6. OBJECTIVE 6: RDB AND ACETATE ADDITION

A goal of this project was to investigate the addition of acetate loading on the system. It was theorized that acetate would act as a source of BOD to increase anaerobic zones and act as a ready electron donor for RDB, but the acetate could also reduce the removal of toluene due to inhibition. Beginning on day 139 an acetate loading rate of 55 mg/day was added to the liquid phase of both reactors in an attempt to facilitate reductive

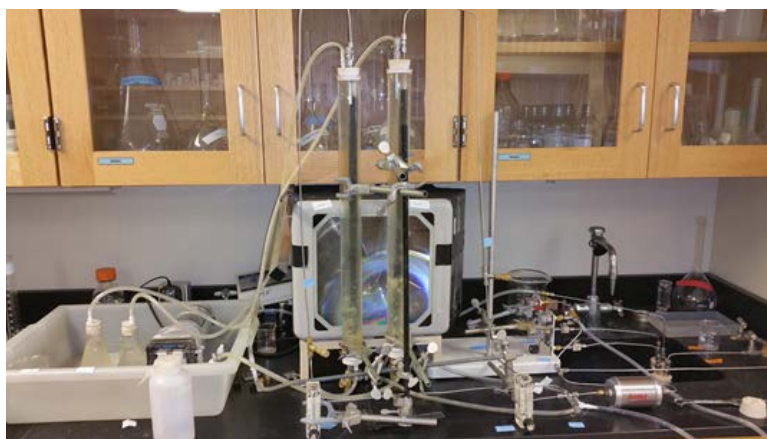
dehalogenation of indigenous biofilm bacteria. During phase II operation no reduction in toluene removal was observed due to the addition of acetate, Figure 5.12. The addition of acetate in the liquid phase at a molar ratio necessary to completely degrade TCE to ethene did not lead to any TCE removal in either bioreactor and no change in DO was observed.

Other dehalogenating bioreactors use an electron donor loading rate significantly higher than the one used in this experiment. Future works should use established loading rates and track the BOD/COD in the system to find optimal operating parameters. Excess acetate could lead to biomass accumulation and higher operating costs.

APPENDIX

Pictures of Biofilm Development and Biofilm Projection

Bioreactor Overview



July 22, 2015 Day Zero. No biofilm development



July 24, 2015. Day 2. Flakes of biofilm on membrane surface



July 26, 2015. Day 4. Membrane surface appears fuzzy, and clumps begin to form



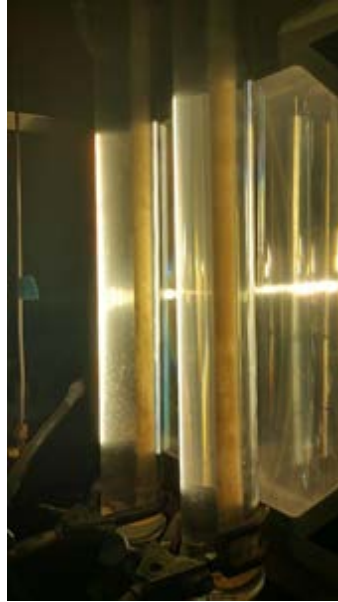
July 27, 2015. Day 5. More biofilm develops and suspended growth is observed



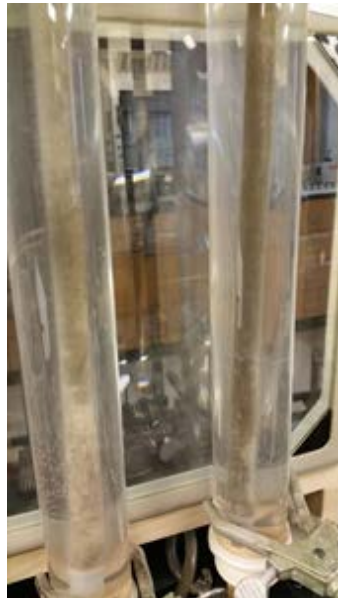
August 3, 2015. Day 13. Biofilm becomes more clumpy and starts to shift to a green color



August 3, 2015. Day 13. Image of biofilm with projector on



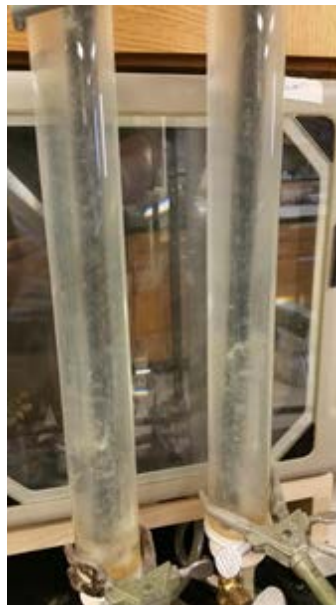
August 4, 2015. Day 14. Biofilm has thicker, fluffy mass



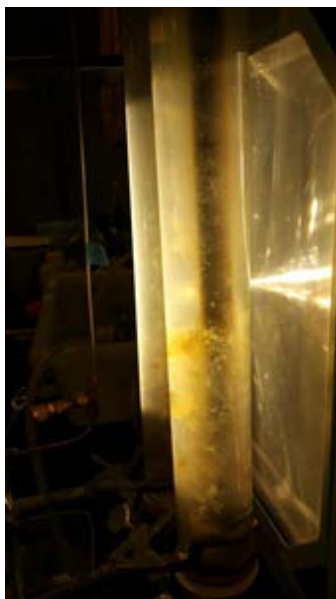
August 27, 2015. Day 37. View of projection on the screen for biofilm thickness measurements



September 28, 2015. Day 69. Shift in biofilm color to black



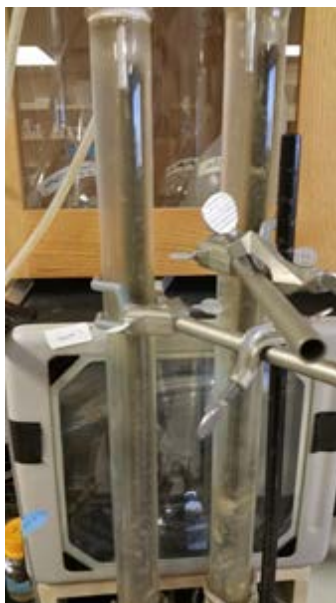
November 11, 2015. Day 113. Projector behind biofilm that shows very thick biofilm
with some suspended growth



November 11, 2015. Day 113. Black inner biofilm with fluffy outer white layer



November 19, 2015. Day 121. Biofilm before the addition of TCE



December 7, 2015. Day 139. Biofilm before the addition of acetate. Reactor two (left) is aerated. Reactor one (right) is not aerated



December 8, 2015. Day 140. Close up of biofilm in reactor two.



December 8, 2015. Day 140. Close up of biofilm in reactor one.



December 20, 2015. Day 152. After aeration in reactor two was shut off and RDB added



December 22, 2015. Day 154. Observed reactor one membrane begin to stretch out



December 28, 2015. Day 160. Both membranes stretched out



BIBLIOGRAPHY

- [1] R. Iranpour, H. H. J. Cox, M. A. Deshusses, and E. D. Schroeder, "Literature review of air pollution control biofilters and biotrickling filters for odor and volatile organic compound removal," *Environmental Progress*, vol. 24, pp. 254-267, 2005.
- [2] S. Mudliar, B. Giri, K. Padoley, D. Satpute, R. Dixit, P. Bhatt, *et al.*, "Bioreactors for treatment of VOCs and odours - A review," *Journal of Environmental Management*, vol. 91, pp. 1039-1054, 2010.
- [3] A. K. Shukla, S. N. Upadhyay, and S. K. Dubey, "Current trends in trichloroethylene biodegradation: A review," *Critical Reviews in Biotechnology*, vol. 34, pp. 101-114, 2014.
- [4] J. E. Burgess, S. A. Parsons, and R. M. Stuetz, "Developments in odour control and waste gas treatment biotechnology: A review," *Biotechnology Advances*, vol. 19, pp. 35-63, 2001.
- [5] O. Suttinun, E. Luepromchai, and R. Müller, "Cometabolism of trichloroethylene: Concepts, limitations and available strategies for sustained biodegradation," *Reviews in Environmental Science and Biotechnology*, vol. 12, pp. 99-114, 2013.
- [6] S. Fetzner, "Bacterial dehalogenation," *Applied Microbiology and Biotechnology*, vol. 50, pp. 633-657, 1998.
- [7] M. D. Lee, J. M. Odom, and R. J. Buchanan Jr, "New perspectives on microbial dehalogenation of chlorinated solvents: Insights from the field," in *Annual Review of Microbiology* vol. 52, ed, 1998, pp. 423-452.
- [8] W. W. Mohn and J. M. Tiedje, "Microbial reductive dehalogenation," *Microbiological Reviews*, vol. 56, pp. 482-507, 1992.
- [9] C. Holliger and W. Schumacher, "Reductive dehalogenation as a respiratory process," *Antonie van Leeuwenhoek*, vol. 66, pp. 239-246, 1994.
- [10] H. Smidt and W. M. De Vos, "Anaerobic microbial dehalogenation," in *Annual Review of Microbiology* vol. 58, ed, 2004, pp. 43-73.
- [11] M. G. Parvatiyar, R. Govind, and D. F. Bishop, "Treatment of trichloroethylene (TCE) in a membrane biofilter," *Biotechnology and Bioengineering*, vol. 50, pp. 57-64, 1996.

- [12] C. E. Aziz, M. W. Fitch, L. K. Linquist, J. G. Pressman, G. Georgiou, and G. E. Speitel Jr, "Methanotrophic biodegradation of trichloroethylene in a hollow fiber membrane bioreactor," *Environmental Science and Technology*, vol. 29, pp. 2574-2583, 1995.
- [13] J. G. Pressman, G. Georgiou, and G. E. Speitel Jr, "A hollow-fiber membrane bioreactor for the removal of trichloroethylene from the vapor phase," *Biotechnology and Bioengineering*, vol. 68, pp. 548-556, 2000.
- [14] Y. Li, B. Li, C. P. Wang, J. Z. Fan, and H. W. Sun, "Aerobic degradation of trichloroethylene by co-metabolism using phenol and gasoline as growth substrates," *International Journal of Molecular Sciences*, vol. 15, pp. 9134-9148, 2014.
- [15] H. Sui, X. G. Li, and S. M. Xu, "Cometabolic microbial degradation of trichloroethylene in the presence of toluene," *Journal of Environmental Sciences*, vol. 16, pp. 487-489, 2004.
- [16] R. L. Ely, K. J. Williamson, M. R. Hyman, and D. J. Arp, "Cometabolism of chlorinated solvents by nitrifying bacteria: Kinetics, substrate interactions, toxicity effects, and bacterial response," *Biotechnology and Bioengineering*, vol. 54, pp. 520-534, 1997.
- [17] M. R. Hyman, S. A. Russell, R. L. Ely, K. J. Williamson, and D. J. Arp, "Inhibition, inactivation, and recovery of ammonia-oxidizing activity in cometabolism of trichloroethylene by *Nitrosomonas europaea*," *Applied and Environmental Microbiology*, vol. 61, pp. 1480-1487, 1995.
- [18] J. Devinny, M. Deshusses, and T. Webster, *Biofiltration for Air Pollution Control*. Washington, D.C: Lewis Publishers, 1999.
- [19] A. Kumar, J. Dewulf, and H. Van Langenhove, "Membrane-based biological waste gas treatment," *Chemical Engineering Journal*, vol. 136, pp. 82-91, 2008.
- [20] M. W. Reij, J. T. F. Keurentjes, and S. Hartmans, "Membrane bioreactors for waste gas treatment," *Journal of Biotechnology*, vol. 59, pp. 155-167, 1998.
- [21] S. J. Ergas, L. Shumway, M. W. Fitch, and J. J. Neemann, "Membrane process for biological treatment of contaminated gas streams," *Biotechnology and Bioengineering*, vol. 63, pp. 431-441, 1999.
- [22] S. J. Ergas and M. S. McGrath, "Membrane bioreactor for control of volatile organic compound emissions," *Journal of Environmental Engineering - ASCE*, vol. 123, pp. 593-598, 1997.

- [23] Z. Wang, J. Ma, C. Y. Tang, K. Kimura, Q. Wang, and X. Han, "Membrane cleaning in membrane bioreactors: A review," *Journal of Membrane Science*, vol. 468, pp. 276-307, 2014.
- [24] I. D. Bo, "Membrane biofiltration of single-compound waste gas streams," PhD, Applied Biological Sciences University of Ghent, Ghent, 2003.
- [25] H. Attaway, C. H. Gooding, and M. G. Schmidt, "Biodegradation of BTEX vapors in a silicone membrane bioreactor system," *Journal of Industrial Microbiology and Biotechnology*, vol. 26, pp. 316-325, 2001.
- [26] E. England, M. W. Fitch, M. Mormile, and M. Roberts, "Toluene removal in membrane bioreactors under recirculating and non-recirculating liquid conditions," *Clean Technologies and Environmental Policy*, vol. 7, pp. 259-269, 2005.
- [27] M. Fitch, J. Neeman, and E. England, "Mass transfer and benzene removal from air using latex rubber tubing and a hollow-fiber membrane module," *Applied Biochemistry and Biotechnology - Part A Enzyme Engineering and Biotechnology*, vol. 104, pp. 199-214, 2003.
- [28] O. Modin, K. Fukushi, F. Nakajima, and K. Yamamoto, "Performance of a membrane biofilm reactor for denitrification with methane," *Bioresource Technology*, vol. 99, pp. 8054-8060, 2008.
- [29] I. Manconi and P. N. L. Lens, "Removal of H₂S and volatile organic sulfur compounds by silicone membrane extraction," *Journal of Chemical Technology and Biotechnology*, vol. 84, pp. 69-77, 2009.
- [30] G. Fuchs, M. Boll, and J. Heider, "Microbial degradation of aromatic compounds-From one strategy to four," *Nature Reviews Microbiology*, vol. 9, pp. 803-816, 2011.
- [31] J. Heider and G. Fuchs, "Anaerobic metabolism of aromatic compounds," *European Journal of Biochemistry*, vol. 243, pp. 577-596, 1997.
- [32] A. M. Spormann and F. Widdel, "Metabolism of alkylbenzenes, alkanes, and other hydrocarbons in anaerobic bacteria," *Biodegradation*, vol. 11, pp. 85-105, 2000.
- [33] R. Chakraborty and J. D. Coates, "Anaerobic degradation of monoaromatic hydrocarbons," *Applied Microbiology and Biotechnology*, vol. 64, pp. 437-446, 2004.

- [34] C. S. Harwood, G. Burchhardt, H. Herrmann, and G. Fuchs, "Anaerobic metabolism of aromatic compounds via the benzoyl-CoA pathway," *FEMS Microbiology Reviews*, vol. 22, pp. 439-458, 1998.
- [35] J. Foght, "Anaerobic biodegradation of aromatic hydrocarbons: Pathways and prospects," *Journal of Molecular Microbiology and Biotechnology*, vol. 15, pp. 93-120, 2008.
- [36] M. T. Amin, S. Hamid, A. A. Alazba, M. N. Amin, M. Islam, and U. Manzoor, "Environmental dynamics and engineered systems for the degradation of trichloroethylene: A critical review," *Global Nest Journal*, vol. 16, pp. 317-329, 2014.
- [37] L. P. Wackett and S. R. Householder, "Toxicity of trichloroethylene to *Pseudomonas putida* F1 is mediated by toluene dioxygenase," *Applied and Environmental Microbiology*, vol. 55, pp. 2723-2725, 1989.
- [38] L. Alvarez-Cohen and P. L. McCarty, "A cometabolic biotransformation model for halogenated aliphatic compounds exhibiting product toxicity," *Environmental Science and Technology*, vol. 25, pp. 1381-1387, 1991.
- [39] H. L. Chang and L. Alvarez-Cohen, "Model for the cometabolic biodegradation of chlorinated organics," *Environmental Science and Technology*, vol. 29, pp. 2357-2367, 1995.
- [40] W. Luo, X. Zhu, W. Chen, Z. Duan, L. Wang, and Y. Zhou, "Mechanisms and strategies of microbial cometabolism in the degradation of organic compounds - Chlorinated ethylenes as the model," *Water Science and Technology*, vol. 69, pp. 1971-1983, 2014.
- [41] A. R. Dolasa and S. J. Ergas, "Membrane bioreactor for cometabolism of trichloroethene air emissions," *Journal of Environmental Engineering*, vol. 126, pp. 969-973, 2000.
- [42] A. Kumar, A. Vercruyssen, J. Dewulf, P. Lens, and H. Van Langenhove, "Removal of gaseous trichloroethylene (TCE) in a composite membrane biofilm reactor," *Journal of Environmental Science and Health - Part A Toxic/Hazardous Substances and Environmental Engineering*, vol. 47, pp. 1046-1052, 2012.
- [43] Y. Zhao, Z. Liu, F. Liu, and Z. Li, "Cometabolic degradation of trichloroethylene in a hollow fiber membrane reactor with toluene as a substrate," *Journal of Membrane Science*, vol. 372, pp. 322-330, 2011.
- [44] T. M. Louie and W. W. Mohn, "Evidence for a chemiosmotic model of dehalorespiration in *Desulfomonile tiedjei* DCB-1," *Journal of Bacteriology*, vol. 181, pp. 40-46, 1999.

- [45] M. Slinger. (2016, Derived copy of Bis2A 06.2 Oxidative Phosphorylation. Available: <http://cnx.org/contents/1LHawezY@1/Derived-copy-of-Bis2A-062-Oxid>
- [46] H. Zhang, M. Ziv-El, B. E. Rittmann, and R. Krajmalnik-Brown, "Effect of dechlorination and sulfate reduction on the microbial community structure in denitrifying membrane-biofilm reactors," *Environmental Science and Technology*, vol. 44, pp. 5159-5164, 2010.
- [47] F. E. Löffler, J. M. Tiedje, and R. A. Sanford, "Fraction of electrons consumed in electron acceptor reduction and hydrogen thresholds as indicators of halorespiratory physiology," *Applied and Environmental Microbiology*, vol. 65, pp. 4049-4056, 1999.
- [48] J. He, Y. Sung, M. E. Dollhopf, B. Z. Fathepure, J. M. Tiedje, and F. E. Löffler, "Acetate versus Hydrogen as Direct Electron Donors To Stimulate the Microbial Reductive Dechlorination Process at Chloroethene-Contaminated Sites†," *Environmental Science & Technology*, vol. 36, pp. 3945-3952, 2002/09/01 2002.
- [49] J. Chung, R. Krajmalnik-Brown, and B. E. Rittmann, "Bioreduction of trichloroethene using a hydrogen-based membrane biofilm reactor," *Environmental Science and Technology*, vol. 42, pp. 477-483, 2008.
- [50] S. Karataş, H. Hasar, E. Taşkan, B. Özkaya, and E. Şahinkaya, "Bio-reduction of tetrachloroethene using a H₂-based membrane biofilm reactor and community fingerprinting," *Water Research*, vol. 58, pp. 21-28, 2014.
- [51] S. C. Popat, K. Zhao, and M. A. Deshusses, "Bioaugmentation of an anaerobic biotrickling filter for enhanced conversion of trichloroethene to ethene," *Chemical Engineering Journal*, vol. 183, pp. 98-103, 2012.
- [52] G. E. Speitel Jr, "Development of bioreactors for the destruction of chlorinated solvents," *Waste Management*, vol. 13, 1993.
- [53] G. E. Speitel and D. S. McLay, "Biofilm reactors for treatment of gas streams containing chlorinated solvents," *Journal of Environmental Engineering (United States)*, vol. 119, pp. 658-678, 1993.
- [54] M. L. Krumme and S. A. Boyd, "Reductive dechlorination of chlorinated phenols in anaerobic upflow bioreactors," *Water Research*, vol. 22, pp. 171-177, 1988.
- [55] D. Frascari, S. Fraraccio, M. Nocentini, and D. Pinelli, "Aerobic/anaerobic/aerobic sequenced biodegradation of a mixture of chlorinated ethenes, ethanes and methanes in batch bioreactors," *Bioresource Technology*, vol. 128, pp. 479-486, 2013.

- [56] M. M. Lorah, C. Walker, and D. Graves, "Performance of an anaerobic, static bed, fixed film bioreactor for chlorinated solvent treatment," *Biodegradation*, vol. 26, pp. 341-357, 2015.
- [57] M. Ziv-El, S. C. Papat, K. Cai, R. U. Halden, R. Krajmalnik-Brown, and B. E. Rittmann, "Managing methanogens and homoacetogens to promote reductive dechlorination of trichloroethene with direct delivery of H₂ in a membrane biofilm reactor," *Biotechnology and Bioengineering*, vol. 109, pp. 2200-2210, 2012.
- [58] J. Chung and B. E. Rittmann, "Simultaneous bio-reduction of trichloroethene, trichloroethane, and chloroform using a hydrogen-based membrane biofilm reactor," in *Water Science and Technology* vol. 58, ed, 2008, pp. 495-501.
- [59] D. Friese, R. Hills, R. Overstreet, and B. Rittmann, "Demonstration and commercialization of ARoNite™, a novel hydrogen-based membrane biofilm biological reduction process," in *Biological Treatment Symposium 2013*, 2013, pp. 252-268.
- [60] A. Ontiveros-Valencia, Y. Tang, R. Krajmalnik-Brown, and B. E. Rittmann, "Perchlorate reduction from a highly contaminated groundwater in the presence of sulfate-reducing bacteria in a hydrogen-fed biofilm," *Biotechnology and Bioengineering*, vol. 110, pp. 3139-3147, 2013.
- [61] Y. Tang, R. Krajmalnik-Brown, and B. E. Rittmann, "Modeling trichloroethene reduction in a hydrogen-based biofilm," *Water Science and Technology*, vol. 68, pp. 1158-1163, 2013.
- [62] Y. Tang, C. Zhou, S. W. Van Ginkel, A. Ontiveros-Valencia, J. Shin, and B. E. Rittmann, "Hydrogen permeability of the hollow fibers used in H₂-based membrane biofilm reactors," *Journal of Membrane Science*, vol. 407-408, pp. 176-183, 2012.
- [63] T. H. Lee, M. Ike, and M. Fujita, "A reactor system combining reductive dechlorination with cometabolic oxidation for complete degradation of tetrachloroethylene," *Journal of Environmental Sciences*, vol. 14, pp. 445-450, 2002.
- [64] J. Gerritse, V. Renard, J. C. Gottschal, and J. Visser, "Complete degradation of tetrachloroethene by combining anaerobic dechlorinating and aerobic methanotrophic enrichment cultures," *Applied Microbiology and Biotechnology*, vol. 43, pp. 920-928, 1995.
- [65] B. Z. Fathepure and T. M. Vogel, "Complete degradation of polychlorinated hydrocarbons by a two-stage biofilm reactor," *Applied and Environmental Microbiology*, vol. 57, pp. 3418-3422, 1991.

- [66] B. Tartakovsky, M. F. Manuel, and S. R. Guiot, "Trichloroethylene Degradation in a Coupled Anaerobic/Aerobic Reactor Oxygenated Using Hydrogen Peroxide," *Environmental Science and Technology*, vol. 37, pp. 5823-5828, 2003.
- [67] D. Volckaert, S. Wuytens, and H. V. Langenhove, "Two phase partitioning membrane bioreactor: A novel biotechnique for the removal of dimethyl sulphide, n-hexane and toluene from waste air," *Chemical Engineering Journal*, vol. 256, pp. 160-168, 2014.
- [68] J. B. Xavier and K. R. Foster, "Cooperation and conflict in microbial biofilms," *Proceedings of the National Academy of Sciences of the United States of America*, vol. 104, pp. 876-881, 2007.
- [69] H. C. Flemming and J. Wingender, "The biofilm matrix," *Nature Reviews Microbiology*, vol. 8, pp. 623-633, 2010.
- [70] P. S. Stewart and M. J. Franklin, "Physiological heterogeneity in biofilms," *Nature Reviews Microbiology*, vol. 6, pp. 199-210, 2008.
- [71] D. De Beer, P. Stoodley, F. Roe, and Z. Lewandowski, "Effects of biofilm structures on oxygen distribution and mass transport," *Biotechnology and Bioengineering*, vol. 43, pp. 1131-1138, 1994.
- [72] L. S. Downing and R. Nerenberg, "Effect of oxygen gradients on the activity and microbial community structure of a nitrifying, membrane-aerated biofilm," *Biotechnology and Bioengineering*, vol. 101, pp. 1193-1204, 2008.
- [73] A. Schramm, D. De Beer, A. Gieseke, and R. Amann, "Microenvironments and distribution of nitrifying bacteria in a membrane-bound biofilm," *Environmental Microbiology*, vol. 2, pp. 680-686, 2000.
- [74] A. C. Cole, M. J. Semmens, and T. M. LaPara, "Stratification of Activity and Bacterial Community Structure in Biofilms Grown on Membranes Transferring Oxygen," *Applied and Environmental Microbiology*, vol. 70, pp. 1982-1989, 2004.
- [75] E. C. England, "Modeling and operation of single and multiple tube membrane bioreactors," *Modeling and Operation of Single and Multiple Tube Membrane Bioreactors*, 2003.
- [76] S. Kim, W. Bae, J. Hwang, and J. Park, "Aerobic TCE degradation by encapsulated toluene-oxidizing bacteria, *Pseudomonas putida* and *Bacillus* spp," *Water Science and Technology*, vol. 62, pp. 1991-1997, 2010.

- [77] C. A. Reddy, T. J. Beveridge, J. A. Breznak, G. A. Marzluf, T. M. Schmidt, and L. R. Snyder, *Methods for General and Molecular Microbiology, Third Edition*: American Society of Microbiology, 2007.
- [78] F. E. Löffler, R. A. Sanford, and K. M. Ritalahti, "Enrichment, cultivation, and detection of reductively dechlorinating bacteria," in *Methods in Enzymology* vol. 397, ed, 2005, pp. 77-111.
- [79] J. E. Amoores and E. Hautala, "Odor as an air to chemical safety: Odor thresholds compared with threshold limit values and volatilities for 214 industrial chemicals in air and water dilution," *Journal of Applied Toxicology*, vol. 3, pp. 272-290, 1983.
- [80] J. Staudinger and P. V. Roberts, "A critical compilation of Henry's law constant temperature dependence relations for organic compounds in dilute aqueous solutions," *Chemosphere*, vol. 44, pp. 561-576, 2001.
- [81] L. M. Freitas dos Santos and A. G. Livingston, "Membrane-attached biofilms for VOC wastewater treatment I: novel in situ biofilm thickness measurement technique," *Biotechnology and Bioengineering*, vol. 47, pp. 82-89, 1995.
- [82] J. Bowman, "The Methanotrophs — The Families Methylococcaceae and Methylocystaceae," in *The Prokaryotes: Volume 5: Proteobacteria: Alpha and Beta Subclasses*, M. Dworkin, S. Falkow, E. Rosenberg, K.-H. Schleifer, and E. Stackebrandt, Eds., ed New York, NY: Springer New York, 2006, pp. 266-289.

VITA

Alexander Korff was born in Fulton, MO on January 19, 1991. In December 2013 he received his B.S. in Environmental Engineering from Missouri University of Science and Technology. In June 2014 he was awarded the Chancellor's Fellowship to pursue his M.S. in Environmental Engineering. In May 2016, Alex graduated with his M.S. in Environmental Engineering from Missouri University of Science and Technology.